



Deposited via The University of Leeds.

White Rose Research Online URL for this paper:

<https://eprints.whiterose.ac.uk/id/eprint/95660/>

Version: Accepted Version

Article:

Richardson, JC, Hodgson, DM, Wilson, A et al. (2016) Testing the applicability of morphometric characterisation in discordant catchments to ancient landscapes: A case study from southern Africa. *Geomorphology*, 261. pp. 162-176. ISSN: 0169-555X

<https://doi.org/10.1016/j.geomorph.2016.02.026>

© 2016, Elsevier. Licensed under the Creative Commons Attribution-NonCommercial-NoDerivatives 4.0 International <http://creativecommons.org/licenses/by-nc-nd/4.0/>

Reuse

Items deposited in White Rose Research Online are protected by copyright, with all rights reserved unless indicated otherwise. They may be downloaded and/or printed for private study, or other acts as permitted by national copyright laws. The publisher or other rights holders may allow further reproduction and re-use of the full text version. This is indicated by the licence information on the White Rose Research Online record for the item.

Takedown

If you consider content in White Rose Research Online to be in breach of UK law, please notify us by emailing eprints@whiterose.ac.uk including the URL of the record and the reason for the withdrawal request.

1 **Testing the applicability of morphometric characterisation in discordant**
2 **catchments to ancient landscapes: a case study from southern Africa**

3 **J.C. Richardson^{1*}, D.M. Hodgson¹, A. Wilson², J.L. Carrivick³ and A. Lang⁴.**

4 *¹School of Earth and Environment, University of Leeds, UK*

5 *²Task Fronterra Geosciences, Perth, Australia*

6 *³ School of Geography and water@leeds, University of Leeds, UK*

7 *⁴ Department of Geography and Geology, Universität Salzburg, Austria*

8 *Corresponding author. Email: eejcr@leeds.ac.uk.

9 **Abstract**

10 The ancient landscapes south of the Great Escarpment in southern Africa preserve
11 large-scale geomorphological features despite their antiquity. This study applies and
12 evaluates morphometric indices (such as hypsometry, long profile analysis, stream
13 gradient index, and linear / areal catchment characteristics) to the Gouritz
14 catchment, a large discordant catchment in the Western Cape. Spatial variation of
15 morphometric indices were assessed across catchment (trunk rivers) and
16 subcatchment scales. The hypsometric curve of the catchment is sinusoidal, and a
17 range of curve profiles are evident at subcatchment scale. Hypsometric integrals do
18 not correlate to catchment properties such as area, circularity, relief, and dissection;
19 and stream length gradients do not follow expected patterns, with the highest values
20 seen in the mid-catchment areas. Rock type variation is interpreted to be the key
21 control on morphometric indices within the Gouritz catchment, especially hypsometry
22 and stream length gradient. External controls, such as tectonics and climate, were

23 likely diminished because of the long duration of catchment development in this
24 location. While morphometric indices can be a useful procedure in the evaluation of
25 landscape evolution, this study shows that care must be taken in the application of
26 morphometric indices to constrain tectonic or climatic variation in ancient landscapes
27 because of inherited tectonic structures and signal shredding. More widely, we
28 consider that ancient landscapes offer a valuable insight into long-term
29 environmental change, but refinements to geomorphometric approaches are needed.

30 *Keywords:* morphometry; ancient landscapes; GIS; rock type

31

32 **1. Introduction**

33 The physiography of South Africa has received much attention owing to its distinctive
34 topography and ancient setting, but the timing and processes involved in landscape
35 evolution remain contentious in several respects. Major river networks within
36 southern South Africa have evolved since the Mesozoic breakup of Gondwana
37 (Moore and Blenkinsop, 2002; Hattingh, 2008), and their development has been
38 synchronous with large-scale (6-7 km) exhumation of the southern African
39 continental crust (Tinker et al., 2008a). However, the tectonic uplift history of
40 southern Africa is poorly constrained, especially the causes and magnitude of uplift
41 (Gallagher and Brown, 1999; Brown et al., 2002; Tinker et al., 2008a; Kounov et al.,
42 2009; Decker et al., 2013). Previous macroscale geomorphological research in
43 southern South Africa has focussed on the formation of the Great Escarpment (e.g.,
44 King, 1953; Partridge and Maud, 1987; Brown et al., 2002), and the development of
45 the Orange River (e.g., Dingle and Hendey, 1984). Furthermore, the timing of the
46 main phase of landscape development in South Africa has been argued to be either

47 Cenozoic (Du Toit, 1937, 1954; King, 1951; Burke, 1996) or Mesozoic (Partridge,
48 1998; Brown et al., 2002; Doucouré and de Wit, 2003; de Wit, 2007).

49 Long-lived ancient landscapes (Bishop, 2007) have been argued for many
50 'Gondwana landscapes' (Fairbridge, 1968) related to large parts of the planet,
51 including cratonic areas and passive continental margins, such as Australia (e.g.,
52 Ollier, 1991; Ollier and Pain, 2000; Twidale, 2007a,b), southern South Africa (e.g.,
53 Du Toit, 1954; King, 1956a), and South America (e.g., King, 1956b; Carignano et al.,
54 1999; Demoulin et al., 2005; Panario et al., 2014; Peulvast and Bétard, 2015). Long-
55 lived landforms and surfaces have also been argued to form parts of Russia
56 (Gorelov et al., 1970), India (Gunnell et al., 2007), Sweden (Lidmar-Bergström,
57 1988), and western France (Bessin et al., 2015). Ancient landscapes have the
58 potential to offer insights into the temporal variation of controls such as tectonic uplift
59 or climate. However, deciphering these factors is problematic within ancient
60 catchments because the imprint of certain forcing factors on catchment morphology
61 may no longer be present owing to long-term erosion. The loss of forcing signals can
62 also be seen with regards to sediment transport, which mediates landscape
63 response (Jerolmack and Paola, 2010). The catchments draining southward from the
64 Great Escarpment in the Western Cape have been subject to cosmogenic (Scharf et
65 al., 2013) and apatite fission track analyses (Tinker et al., 2008a) to determine rates
66 of fluvial erosion and exhumation, respectively; but these data have not been
67 through a detailed geomorphological assessment (Rogers, 1903; Partridge and
68 Maud, 1987). Fundamental morphometric analyses of South African drainage basins
69 have yet to be attempted, although this approach has the potential to yield insights
70 into the long-term landscape evolution as shown by the Walcott and Summerfield
71 (2008) hypsometry study in the Eastern Cape.

72 Geomorphometry employs a range of morphometric indices to help characterise the
73 history of a drainage basin (Horton, 1932; Miller, 1953; Schumm, 1956; Chorley,
74 1957; Strahler, 1964). Morphometric indices include river network analysis,
75 hypsometry, and analysis of the stream profile. River networks are used to infer the
76 tectonic and climatic history of a region (e.g., Montgomery et al., 2001; Walcott and
77 Summerfield, 2008; Antón et al., 2014), as river form is closely linked to these
78 extrinsic factors. However, river networks are also governed by intrinsic factors such
79 as network reorganisation through stream capture (Davis, 1889), bedrock geology
80 (Tinkler and Wohl, 1998; Duvall et al., 2004), and sediment flux (Richards, 1982;
81 Sklar and Dietrich, 2001). Many studies of morphometric indices relate to tectonically
82 active areas (e.g., Snyder et al., 2000; Zhang et al., 2013; Antón et al., 2014; Ghosh
83 et al., 2014). However, these indices are rarely applied to tectonically quiescent
84 areas or ancient landscapes. An example of a morphometric approach to ancient
85 landscape development is by Walcott and Summerfield (2008) who assessed the
86 variation in hypsometric integral within catchments draining the Drakensberg
87 mountain range in eastern South Africa. They argued that variation in hypsometric
88 integral within streams of order 5 or less is because of differences in bedrock type
89 resistance as well as moderate crustal displacement, whereas the larger stream
90 orders (>6) are independent of rock type or tectonic control.

91 In this study, we test if morphometric indices can offer further insight into the history
92 of the understudied ancient landscapes of southern South Africa, which have
93 undergone reorganisation because of the exhumation of the resistant Cape Fold Belt
94 and retreat of the Great Escarpment. Therefore, inherited structures are expected to
95 play an important role in landscape evolution of the Gouritz catchment. We aim to
96 address the following objectives: (i) to extract morphometric indices for an

97 antecedent and tectonically quiescent drainage basin, the Gouritz Catchment; (ii) to
98 document spatial variation in morphometric indices within the main tributaries; (iii) to
99 test the prevailing conceptual models in the literature of external (e.g., Montgomery
100 et al., 2001; Keller and Pinter, 2002; Manjoro, 2015) and internal controls (e.g.,
101 Tooth et al., 2004; Walcott and Summerfield, 2008; Jansen et al., 2010) on
102 geomorphometry and landscape evolution; and (iv) to assess the broader suitability
103 of morphometric indices for characterisation of ancient landscapes.

104 **2. The Gouritz catchment**

105 The Gouritz catchment is located within the Western Cape Province of South Africa
106 (Fig. 1) and is one of several antecedent systems draining from the Great
107 Escarpment that cut across the west-east trending Cape Fold Belt (CFB) mountains
108 to the Atlantic and Indian Oceans. Antecedence in the Western Cape is shown by
109 the large-scale discordance of the main trunk rivers (Rogers, 1903), which
110 completely dissect the resistant CFB and have deeply incised meanders into
111 quartzites (up to 1 km in depth). The main catchment evolutionary events include the
112 breakup of Gondwana in the Mesozoic (Summerfield, 1991; Goudie, 2005) and the
113 large-scale incision in the Cretaceous resulting in the exhumation of the CFB (Tinker
114 et al., 2008a) and the Karoo basin-fill. As such, the retreat and development of the
115 Great Escarpment (Fleming et al., 1999; Cockburn et al., 2000; Brown et al., 2002;
116 Moore and Blenkinsop, 2006) has an important control on catchment evolution and
117 stream capture of the Orange River catchment. King's (e.g., King, 1963, 1972) view
118 of the escarpment forming at the coastline and retreating uniformly since the
119 breakup of Gondwana has been disproved by numerical models (e.g., Gilchrist and
120 Summerfield, 1990; van der Beek et al., 2002) and dating techniques (e.g., Fleming

121 et al., 1999; Brown et al., 2002). On the basis of apatite fission track data,
122 researchers have proposed that the Great Escarpment has retreated a *maximum* of
123 29 km to its current position since the Cretaceous (Brown et al., 2002), which would
124 have affected the headwaters of the Gouritz catchment.

125

126 The Gouritz catchment has an area of 6.45×10^4 km² and a stream order of 7
127 (Strahler, 1957). The basin is composed of six main tributaries: the Traka, Touws,
128 Buffels, Olifants, Dwyka, and Gamka rivers (Fig. 1). The source regions for many of
129 the main tributaries are hillslopes to the south of the Great Escarpment, with the
130 Gouritz system reaching the ocean at Gouritzmond (Fig. 1). The majority of the rivers
131 are bedrock or mixed bedrock-alluvial in nature, with common steep-sided valleys
132 and bedrock-confined gorges.

133 The Great Escarpment separates an interior plateau of low relief and high elevation
134 from a coastal region of high relief and low average elevation (Fleming et al., 1999;
135 Tinker et al., 2008b; Moore et al., 2009). The Gouritz catchment also contains a
136 segment of the exhumed CFB, which is a compressional mountain range that formed
137 in the late Permian and Triassic (Tankard et al., 2009; Flint et al., 2011).

138 Physiographically, and based on variation in elevation and landscape morphology,
139 the drainage basin can be divided into the following units: escarpment, central
140 Karoo, Cape Fold Belt, and coastal (Fig. 2A). The application of Hammond's
141 topographic analysis (Fig. 2B) to the Gouritz catchment reveals that the area is
142 dominated by (i) plains that usually carry a thin (<1 m) sedimentary cover, which
143 decreases toward the north, and that include dissected pediment surfaces; and (ii)
144 mountains where bedrock crops out in the CFB and escarpment regions with a thin
145 regolith, if present.

146 The present day climate of the Gouritz catchment is primarily semiarid (Dean et al.,
 147 1995) with mean annual precipitation of 262 mm (CSIR, 2007). The region has a
 148 clear split between summer and winter rainfall regimes, with late summer to winter
 149 rainfall in the Great Escarpment and central Karoo region, winter rainfall in the
 150 western CFB, late summer to winter rainfall in the southern CFB, and summer and
 151 winter rainfall in the coastal areas (CSIR, 2007). The lower part of the catchment in
 152 the coastal region has a Mediterranean-type climate (Midgley et al., 2003).
 153 Orographic rainfall over the CFB provides much of the discharge (Midgley et al.,
 154 2003), with the other main source being intense thunderstorms that usually form on
 155 the escarpment and move south over the central Karoo. Smaller tributaries in the
 156 upper reaches of many of the larger trunk rivers are ephemeral. South of the CFB,
 157 trunk rivers are perennial with the main tributaries transporting boulders to sand-
 158 grade material as bedload, although no sediment transport data is available. The
 159 climatic history of southern South Africa is poorly constrained. Since the Cretaceous
 160 (and the development of the major drainage systems), we see a general trend
 161 toward a more arid environment (Bakker and Mercer, 1986), with variation in
 162 intensity in the winter or summer rainfall regime (Bar-Matthews et al., 2010) as well
 163 as the fire regime (Seydack et al., 2007).

164 The substrate of Gouritz catchment is predominantly Palaeozoic rocks of the Cape
 165 and Karoo Supergroups, composed of various mudstone and sandstone units (Fig.
 166 1). Small inliers of the Kansa Group (conglomerate, shale, mudstone) are found in
 167 the CFB. Resistant lithologies (Fig. 3) within the Gouritz catchment include the
 168 Precambrian Congo Cave Group, which comprises metasediments (limestones,
 169 arenites, mudrocks), the Table Mountain Group quartzites, and Jurassic dolerite
 170 intrusions dominantly toward the north and granite plutons in coastal areas of the

171 catchment (Fig. 1). The Mesozoic Uitenhage Group comprised mainly of
172 conglomeratic and sandy units represents the youngest resistant rock type within the
173 basin.

174 The structural geology of the drainage basin is dominated by large-scale (~11 km
175 wavelength; Tankard et al., 2009) E-W trending folds that decrease in amplitude
176 toward the north (Paton, 2006, Spikings et al., 2015). The folds formed along the
177 southwestern margin of Gondwana during Paleozoic-Mesozoic convergence (e.g.,
178 Tankard et al., 2009). The Gouritz catchment contains two large anticlines, the
179 Swartberg and Langeberg (CFB), which are cut by large Mesozoic normal faults
180 (Paton, 2006), the Swartberg and Worcester faults, respectively (Fig. 1).

181 The Gouritz catchment is currently tectonically quiescent, with a lack of fault scarps,
182 low seismicity (Bierman et al., 2014), and low rates of sediment supply (Kounov et
183 al., 2007; Scharf et al., 2013). The tectonic history of the area is contentious
184 (Gallagher and Brown, 1999; Brown et al., 2002; Tinker et al., 2008a; Kounov et al.,
185 2009; Decker et al., 2013). Researchers have debated about the events causing the
186 large-scale denudation in the Cretaceous, with ideas often related to plume activity in
187 the early Cretaceous (Moore et al., 2009). Burke (1996) proposed that the most
188 recent uplift occurred around 30 Ma ago because of a thermal anomaly, whereas
189 Partridge and Maud (1997) argued for a later period of activity in the Miocene (~250
190 m uplift) and again in the Quaternary (900 m uplift). The large-scale exhumation
191 across southern South Africa could still be driving epeirogenic uplift (Tinker et al.,
192 2008a).

193 **3. Methodology**

194 Catchment topography from a digital elevation model (DEM) based on ASTER (30
195 m) data, was reprojected into WGS 1984 world Mercator coordinates. Catchment
196 boundaries were extracted using the default hydrology toolbox in ArcGIS 10.1, in
197 which the DEM was manually filled in order to remove any holes within the DEM to
198 allow for flow path extraction. Following Abedlkareem et al. (2012) and Ghosh et al.
199 (2014), a minimum upstream drainage area threshold of 3.35 km² was used to
200 delineate the drainage network, showing perennial and ephemeral rivers.
201 Stratigraphic unit, rock type, and structural geological data sets were obtained
202 digitally from the Council of Geoscience, at a scale of 1:250,000.

203 *3.1. Drainage characterisation and landforms*

204 Zernitz (1932) laid the foundation of drainage pattern analyses, argued that structure
205 and slope determine the spatial arrangement of rivers, and determined six river
206 patterns (dendritic, trellis, rectangular, radial, annular, and parallel). A more refined
207 classification was provided by Howard (1967) with additional subclassifications,
208 which included subdendritic, pinnate, anastomotic, and distributary. Drainage
209 patterns are fundamental in determining structural change at a local and regional
210 scale (Hills, 1963) with analyses used primarily in tectonic settings (e.g., Gupta,
211 1997; Friend et al., 2009).

212 The drainage pattern of the Gouritz Catchment was assessed and assigned
213 drainage categories in order to assess controls on the catchment (Zernitz, 1932) at a
214 regional scale (Knighton, 1998). The impact of tectonic structures is shown by the
215 dominance of trellis or parallel patterns. Tectonic structure has been shown to be
216 important in catchments draining the western domain of the CFB (Manjoro, 2015):
217 49% of the catchment area of the Gouritz drains the southern domain of the CFB.

218 *3.2. Morphometric indices*219 *3.2.1. Long profile*

220 Long profiles of the main trunk rivers were extracted using ArcGIS by digitising the
221 stream network with 10-m vertical spacing along the stream. Assessing long profiles
222 of rivers allows quantitative analysis of fluvial incision and lithological controls (Hack,
223 1973). The analysis of long profiles can highlight knickpoints, which are the principal
224 method of channel lowering within bedrock channels (Whipple, 2004). In this study,
225 long profiles were further quantified using the stream gradient index (Hack, 1973),
226 which would be expected to be approximately constant along a graded long profile in
227 a homogenous lithology. Deviations from the average value were therefore assumed
228 to be caused by forcing factors (Antón et al., 2014) such as tectonics (Keller and
229 Pinter, 2002), lithology (Hack, 1973), or migrating knickpoints (Bishop et al., 2005).

230 *3.2.2. Stream gradient index*

231 Long profile geometry was used to assess the level of grading within a river by
232 employing the stream gradient index (SL; Hack, 1973) and was calculated as

233
$$SL = (\Delta H / \Delta Lr) \Delta Lsc \quad (1)$$

234 where ΔH is change in altitude, ΔLr is length of the reach, and ΔLsc is the horizontal
235 flow path length from the watershed divide to the midpoint of the reach. The stream
236 length gradient was calculated in 50-m reaches for the main trunk rivers, the data
237 were then normalised (to a value between zero and one, using the range of values
238 collected from all trunk rivers) to allow comparison between the trunk rivers.

239 *3.2.3. Morphometric indices*

240 Morphometric indices permit the quantitative assessment of, and comparison
241 between, landscapes and can highlight anomalies along the river network. Linear

242 measurements such as stream order, stream length, and bifurcation ratio (Horton,
243 1945) were extracted using ArcGIS. Areal measurements such as basin area,
244 drainage density (Horton, 1945), and circularity (the ratio of the perimeter of the
245 basin to the perimeter of a circle with the same area) were also extracted. Drainage
246 density was extracted for the entire catchment and also for the main rock types
247 within the catchment (Fig. 1) in order to assess the impact of different bedrock
248 resistances to the drainage pattern.

249 *3.2.4. Hypsometry*

250 Hypsometry describes the area distribution of elevation within a catchment. Strahler
251 (1952) defined the hypsometric integral (HI) as the differences in sinuosity of curve
252 form and the proportionate area below the curve. Strahler (1952) argued that
253 catchments where $HI > 0.6$ are in disequilibrium (youth) and the catchment shows
254 rapid slope transformation as the drainage system expands, and where HI is
255 between 0.4 and 0.6 catchments are in equilibrium (mature). Below 0.4 the
256 catchments are argued to be in a monadnock phase (old age; Strahler, 1952). More
257 recently hypsometry has been used for a wide range of applications, including the
258 evolution of landscapes (Hancock and Willgoose, 2001), the effect of climate
259 (Montgomery et al., 2001), and the influence of tectonics on catchments (Ohmori,
260 1993). Hypsometric curves have been used to decipher the forcing factors in
261 catchments (Strahler, 1952; Montgomery et al., 2001; Walcott and Summerfield,
262 2008). However, the influence of drainage basin properties such as area, circularity,
263 relief, and dissection on the HI has received mixed results, with researchers arguing
264 for correlation (Hurtrez et al., 1999; Chen et al., 2003) and no correlation (Walcott
265 and Summerfield, 2008). Strahler (1952) argued that catchments try to maintain a

266 convex or sinusoidal curve, with erosion of the transitory concave monadnock phase
267 returning the curve to a sinusoidal curve.

268 In this study, hypsometric data (hypsometric integral (Eq. 2) and curve) were
269 extracted by an ArcGIS tool (Hypsometric Tools by Davis, 2010) for the whole
270 catchment and then western-draining subcatchments. The western-draining
271 catchments are defined as those that drain the western part of the Gouritz
272 catchment, delineated at the confluence with the main trunk river (Gamka River).
273 These subcatchments were chosen to investigate the variation in hypsometric
274 integral and curve shape with respect to the location of the catchment and the
275 stream order. Only analysing the western-draining subcatchments is justified
276 because the Gouritz catchment is nearly symmetrical (Fig. 1) and because the
277 geology is broadly similar in the western and eastern portions of the catchment (Fig.
278 1). Hypsometric integrals were then compared to basin properties including
279 circularity, area, relief (Eq. 3), dissection (Eq. 4), and key rock types and geological
280 structure.

$$281 \quad H.I. = \frac{\text{mean elevation} - \text{minimum elevation}}{\text{maximum elevation} - \text{minimum elevation}} \quad (2)$$

$$282 \quad \text{Relief} = \text{maximum elevation} - \text{minimum elevation} \quad (3)$$

$$283 \quad \text{Dissection} = \text{mean elevation} - \text{minimum elevation} \quad (4)$$

284 **4. Results**

285 *4.1. Catchment characteristics*

286 Overall, the Gouritz catchment exhibits a dendritic drainage pattern (Fig. 1), but
287 spatial variation is seen within the subcatchments in different physiographic regions.
288 Dendritic patterns are present within the central Karoo and escarpment regions,

289 where the Karoo Supergroup crops out, which is an area dominated by irregular
290 plains with low relief (Fig. 2B). Within the CFB, trellis drainage patterns are found
291 (Fig. 4A). The coastal region is dominated by small dendritic catchments (Fig. 4A).
292 The Gouritz catchment is a stream order 7 catchment (Strahler, 1952) and has a
293 drainage density of 0.454 km/km². Drainage density is lowest on quartzite bedrock,
294 the most resistant rock type (Fig. 3), and is the highest on the more easily eroded
295 Karoo Supergroup sandstones and mudstones (Table 1). Physiographically, the
296 CFB- and escarpment-draining subcatchments have the greatest variation in
297 elevation. The CFB is dominated by streams of a lower order which drain the
298 majority of the slopes, with the high order (>4) streams cutting straight through the
299 mountain chain. The lower order streams (<3) are normally straight with meandering
300 dominating in stream order >4 (Fig. 4). Deeply incised meander bends are found in
301 some of the main trunk rivers that cut across the CFB, e.g. Gamka-Gouritz River.
302 Several rivers show right angles in their courses and evidence of beheading (Figs.
303 4B, C) and are remnants of stream capture sites, of which many are expected in
304 such a long-lived catchment. The mean bifurcation ratio of the catchment is 3.39;
305 however, variation within individual stream orders is seen, with a range from 2 to 6.

306

307 *4.2. Morphometric indices*

308 *4.2.1. Long profiles*

309 The long profiles of the main tributaries of the Gouritz catchment show a lack of
310 single-graded form. Overall, the long profiles are concave in the headwater regions
311 and fairly straight in the CFB (Fig. 5). Concave long profiles are mainly found in the
312 physiographic regions of the Great Escarpment and central Karoo regions but are
313 also found in the transverse Olifants and Traka rivers whose headwaters form in the

314 Cape Fold Belt (Fig. 5). Knickpoints are present along the long profiles (Fig. 5),
315 which in some cases relate to artificially dammed lakes. These dams were
316 preferentially sited at the upstream side of narrow canyons, with the knickpoints
317 corresponding to lithostratigraphic boundaries between quartzite and other Cape
318 Supergroup rock types or the Uitenhage Group. Dolerite intrusions (Dwyka and
319 Gamka rivers) do not always exhibit knickpoints. A detailed study of the Swartberg
320 mountains indicates that in the smaller mountain-draining catchments (stream order
321 <3) knickpoints are prevalent and commonly are tied to lithostratigraphic boundaries
322 involving quartzite (Figs. 3, 6).

323 *4.2.2 Stream gradient index*

324 Figure 6 shows the variation of stream gradient indices within the Gouritz catchment.
325 The data were normalised with a value of 1 indicating high stream gradients; a full
326 range of SL are seen within the catchment. The headwaters of all the trunk rivers
327 have low SL, with values below 0.2, which is exceptionally low and shows an
328 increase downstream. The rivers that cross the central Karoo (Buffels, Gamka, and
329 Dwyka rivers) show gradients between 0 and 0.4. This area is characterised by flat
330 plains and is dominated by the relatively easily eroded Karoo Supergroup rock types.
331 The CFB, which all the main trunk rivers either run parallel to or transverse (Fig. 1),
332 shows the highest variation in SL, with values between 0.2 and 1. The CFB is
333 dominated by the Cape Supergroup, with resistant quartzites and metamorphosed
334 sandstones as well as the resistant Uitenhage Group and Cango Cave Group rock
335 types. Stream gradient indices then decrease in the coastal region with the SL of the
336 majority of reaches below 0.2, where the Cape Supergroup outcrops are dominated
337 by mudstones. Stream gradient is unaffected by large-scale faults (mapped at
338 1:25,000).

339 4.2.3. *Hypsometry*

340 The hypsometric integral of the Gouritz catchment is 0.34, and the hypsometric
341 curve for the catchment is sinusoidal (Fig. 7). The overall drainage basin has a
342 circularity of 0.16, which indicates the drainage basin shape is highly irregular. In
343 order to understand how hypsometry varies throughout the drainage basin, the
344 western-draining catchments of the main trunk river (Gamka River) were assessed in
345 detail.

346 Western-draining catchments range in stream order from 1 to 6 and have a mean
347 basin area of 728.10 km² (ranging from 4.37 to 19,054.91 km²). In Fig. 8,
348 hypsometric integrals are plotted against catchment characteristics. The R^2 value
349 shows no correlation between the hypsometric integral and each variable:
350 hypsometric integral and circularity = 0.0053, hypsometric integral and area =
351 0.0872, hypsometric integral and dissection = 0.0321, and hypsometric integral and
352 relief = 0.1761. The hypsometric integral, therefore, appears to be independent of
353 catchment factors. The hypsometric integral on average decreases with increasing
354 stream order (Table 3). The central Karoo catchments have the highest mean
355 hypsometric integral, and the coastal catchments the lowest (Table 4).

356 Some patterns between stream order and geomorphological location are apparent.
357 Catchment area increases with stream order, with larger basins having lower
358 hypsometric integrals (Fig. 8A). Higher order streams (>4) on average have a lower
359 circularity and data is less scattered than lower order streams (<3; Fig. 8B). The
360 lower circularity value of higher stream order catchments relates to a more
361 complicated drainage network and watershed shape. Lower order streams (<3) have
362 a wider range of dissection and relief (Figs. 8C, D); this seems to be a function of
363 location with many of these streams draining the CFB. The central Karoo catchments

364 are more homogenous and less scattered, with low levels of dissection and relief,
365 and the area is characterised by large flat areas (Fig. 2B). The escarpment
366 represents the headwaters of many of the central Karoo catchments, and only
367 represents a small proportion of the total catchment area. Hypsometric integrals do
368 not correlate with the distance of the catchment from the river mouth (Fig. 8E; $R^2 =$
369 0.05). Figure 8E also shows how the range of integrals decreases toward the
370 escarpment, whilst the drainage density increases (i.e., density of data points
371 increases).

372 *Hypsometric curves:* The hypsometric curves from subcatchments within the Gouritz
373 catchment can be classified as sinusoidal, straight, concave, and convex (Fig. 9A).
374 Overall, the Gouritz catchment has a sinusoidal curve (Fig. 7), whereas at
375 subcatchment scale, the majority of curves are concave (Fig. 9A). The concave
376 curves can be seen in a range of stream orders (stream order 1 to 6), whereas the
377 convex, straight, and sinusoidal catchments are associated with the lower stream
378 orders (<3) (Fig. 9). No systematic variation in the curve shape is seen toward the
379 escarpment (Fig. 9B) or within each geomorphological region.

380 Curve shapes were quantified to assess whether the observed variation could be
381 attributed to internal or external catchment controls. Figure 9C shows the percentage
382 area of the catchment that lies below half the maximum elevation within the western-
383 draining catchments. The more dissected a basin is, the higher the area of the
384 catchment below the maximum value within the basin. The coastal catchments are
385 highly dissected, with the majority of catchments having >90% of area lower than
386 50% of the maximum height. The CFB has similar levels of dissection where many
387 catchments have >80% of area lower than 50% of the maximum height. Dissection
388 also increases toward the escarpment where, on average, the lowest percentage of

389 area below 50% of the maximum height is within the central Karoo catchments,
390 where average elevation is high and slope angles are low.

391 Figure 10 shows the influence of rock type on hypsometric curves of stream order 1
392 to 6 streams. The presence of resistant rock types (Fig. 3), such as the Cango Cave
393 Group and igneous intrusions at the higher elevations of the catchment, allows
394 elevation to be preserved causing a disturbance of the hypsometric curve. The
395 hypsometric curve in these locations has a lower slope than the catchments without
396 resistant rock types, with a higher proportion of area preserved in the higher
397 elevations (e.g. Figs. 10A, E). Hypsometric curve slope also decreases when
398 resistant rock types are found at lower elevations (e.g. igneous intrusions,
399 Uitenhage, and Cango Cave groups; Fig. 10D). At the lower elevations of
400 catchments the influence of resistant rock types decreases, e.g. below 50% of the
401 maximum elevation, especially in the larger catchments. The presence of quartzite
402 does not impact the curve shape significantly (Figs. 10C, D). Curve shape variation
403 within catchments dominated by the Karoo Supergroup cannot be attributed to
404 different rock types, although the lithostratigraphic groups within the Karoo
405 Supergroup have different proportions of mudstone and sandstone (Fig. 10B). Some
406 catchments have a large change in slope at the lower elevations (Figs. 10D, F),
407 which does not correspond to a change in the proportions of rock type.

408 **5. Discussion**

409 When assessing the dominant controls on the development of an ancient landscape,
410 uncertainty remains in the timing and effects of external forcing factors; and the long
411 timescales involved mean that external signals can be overprinted. Nonetheless, the

412 Gouritz catchment is an ideal test of a morphometric approach to considering the
413 dominant controls on the evolution of long-lived drainage basins.

414 *5.1. Impact of bedrock type*

415 The impact of bedrock type is seen in the hypsometric curves, where the high relief
416 of some subcatchments is related to the resistant dolerite intrusions and Cango
417 Cave Group bedrock (Figs. 3, 10A, E). The deviation in curves dominated by the
418 Cape (including quartzites) and Karoo supergroups cannot be related to rock type,
419 and the resistance of the units appears to be fairly similar (Fig. 3). However,
420 parameters such as bed thickness, bed orientation (strike and dip), and the extent of
421 jointing – which have not been taken into account in this study – also impacts the
422 resistance of bedrock to erosion (Walcott and Summerfield, 2008). Cape Supergroup
423 rocks have also been metamorphosed, which can cause rocks of different
424 compositions to have more similar resistance to erosion (Zernitz, 1935).

425 The level of dissection within catchments as shown by the hypsometric curves can
426 also be attributed to variation in bedrock type; many of the coastal catchments are
427 underlain by mudstones (Bokkeveld Group, Cape Supergroup), which are more
428 easily eroded (Fig. 3), resulting in a concave curve. The CFB-draining
429 subcatchments are dominated by resistant metamorphosed bedrock, associated with
430 lower rates of erosion (Scharf et al., 2013) and, therefore, a longer duration of
431 evolution resulting in sinusoidal or straight curves (Figs. 9A, B). In the CFB area, the
432 catchments are lower order streams (<3), and the impact of bedrock type appears to
433 be more dominant (Fig. 4A). The wide range in circularity values in the CFB-draining
434 subcatchments also indicates a larger structural and lithological control within these
435 mountainous catchments (Fig. 8A).

436 The impact of bedrock type appears to be stream-order dependent; knickpoints are
437 pinned to contacts between rock types of different resistance within the
438 subcatchments (Fig. 6). The large trunk rivers do not show this relationship as such
439 pronounced changes in stream profile, which could be a function of temporal
440 development; however, the profiles are straighter in the CFB area because of the
441 high rock resistance (Figs. 3, 5). Bedrock type also impacts on drainage densities.
442 The Karoo Supergroup rocks have the highest drainage densities (Table 1), and
443 these rocks have been less affected by burial metamorphism. The more resistant
444 rocks have lower drainage densities owing to the time taken for incision and the
445 formation of a drainage network. Dolerite has been shown to play a key role in
446 catchment development within South Africa (Tooth et al., 2004). In the upper Gouritz
447 catchment, where dolerite is dominantly found, low stream gradients are present and
448 the impact differs from Tooth et al. (2004) as the dolerite intrusions are not always
449 represented as knickpoints along the long profile (Fig. 5). This could be because of
450 the limited thickness of the dolerite intrusions in the Gouritz catchment in comparison
451 to those exhumed in the South African Highveld (Tooth et al., 2004).

452 Quartzite has been argued to be the most dominant rock type on catchment
453 dynamics (Jansen et al., 2010); however, in this study the presence of quartzites
454 does not always vary morphometric indices. Typically, high SLs are located in the
455 upper reaches of catchments (Antón et al., 2014); however, this is not the case for
456 the Gouritz catchment (Fig. 6). The highest values are seen within the CFB, with low
457 values at headwater regions. The highest values of SL are not always associated
458 with the rivers crossing quartzitic lithologies, but mainly with the Uitenhage Group.
459 When assessing the major trunk streams at reach level, quartzite does not have
460 strong control. This is because the main trunk rivers breach the quartzite in only

461 seven locations (Fig. 6), where deeply dissected gorges have formed resulting in
462 high gradients and meandering in these locations. The majority of the river courses
463 transverse other rock types such as the resistant Cango Cave Group, where high
464 stream gradients and meanders are present (Fig. 6). The large degree of variation in
465 stream length gradient within the Cape Supergroup rock types could be explained by
466 the variation of bed thickness, bedding orientation, and jointing, as well as the
467 degree of metamorphism.

468 *5.2. Impact of inherited tectonic structures*

469 The impact of tectonic structures within the Gouritz catchment is primarily exhibited
470 in the drainage pattern of the lower order streams (order 2 and 3; Fig. 4A).

471 Bifurcation ratios above 5 normally indicate a structural control (Strahler, 1957).

472 However, in the case of the large trunk rivers of the Gouritz catchment (stream order
473 4 and 6), the higher stream orders dissect the CFB and are not directed or deflected
474 by the E-W trending structures; this discordance supports their interpretation as
475 antecedent systems (Rogers, 1903). Additional evidence of antecedence is shown
476 by the combination of high gradients and meander forms into resistant lithologies
477 within the CFB (Fig. 3). The CFB folds have the greatest control on subcatchments;
478 this is especially evident in a stream order 2 river in Fig. 4B that has a linear
479 planform and stream order 3 rivers in Fig. 4A. The strong structural control within the
480 catchment with regards to bifurcation ratio is, therefore, the antecedence of the
481 major tributaries (Rogers, 1903), which explains the higher bifurcation ratios in
482 stream order 4 and 6 streams.

483 Across the catchment, the CFB represents a large proportion of elevation resulting in
484 the plateau in the hypsometric curve (Fig. 7). The CFB has low rates of erosion, with
485 the resistant rock types allowing the post-orogenic feature to persist (Scharf et al.,

486 2013). Additional preservation of elevation is caused by the widespread presence of
487 fossilised plains, pediments (Kounov et al., 2015), and presence of the Great
488 Escarpment (Fig. 2B). Exceptionally low SL in the ephemeral headwaters indicates
489 the importance of the flat top nature of the Great Escarpment (Fig. 2B). South Africa
490 formed a central part of Gondwana and was a super-elevated continent (Patridge
491 and Maud, 1987; Rust and Summerfield, 1990); during rifting in the Mesozoic,
492 reorganisation of seaward-draining catchments such as the Gouritz occurred. The
493 headwaters of the Gouritz incised the escarpment face and now drain a portion of
494 the flat area on the escarpment inherited from the breakup of Gondwana. The
495 concave nature of the headwaters shown in the long profiles (Fig. 5) indicates the
496 large change in elevation between the flat top of the Great Escarpment and the
497 central Karoo, which sits ~700 m below the escarpment.

498 Large-scale extensional faults (Fig. 1) do not appear to have an important control
499 within the catchments, either within the hypsometric curves or the morphometric
500 indices. However, the rock types within the catchment, especially the CFB, are
501 pervasively jointed and faulted, and therefore, must be an important control at a
502 small scale (Manjoro, 2014).

503 *5.3. Large-scale forcing factors*

504 Variation in morphometric indices (circularity, SL, and hypsometry) indicate that the
505 Gouritz catchment has had a complicated development history (Fig. 11). Commonly,
506 hypsometric curves are used to elucidate large-scale forcing factors in catchments
507 (Montgomery et al., 2001). The sinusoidal shape of the Gouritz catchment (Fig. 9) is
508 often related to rejuvenation (Ohmori, 1993). The uplift in South Africa is contentious
509 (Gallagher and Brown, 1999; Brown et al., 2002; Tinker et al., 2008a; Kounov et al.,
510 2009; Decker et al., 2013), however Walcott and Summerfield (2008) argued that if

511 tectonic activity did occur within South Africa, it was either at a low rate or a long
512 time ago because the hypsometry of the catchments are concave-up with low
513 integral values, and the tectonic pulse is no longer expressed physiographically (Fig.
514 11). Summerfield (1991) related sinusoidal curves extracted from rivers in South
515 Africa to coastal upwarp. The lower curve portion of the Gouritz catchment is not
516 underlain by resistant lithologies, and the sinuous nature at these low elevations
517 could be related to coastal upwarp. Strahler (1952) argued that fluvial equilibrium is
518 shown by hypsometric integrals between 0.4 and 0.6. However, this is not always the
519 case, as shown by this study, and caution is needed in the application of
520 hypsometric integrals.

521 In the western-draining catchments, many of the hypsometric curves are convex,
522 with variation in shape occurring in adjacent catchments. This suggests that either
523 different forcing factors are affecting the catchments or they are reacting to the same
524 forcing factors in different ways. Within smaller subcatchments, stream capture has
525 been shown to cause rejuvenation and can occur as an allogenic process (Prince et
526 al., 2011). Stream capture can explain the variation in some of the subcatchments;
527 however, it is not sufficient to explain such large-scale processes for the entire
528 drainage basin.

529 Hurtrez et al. (1999) and Chen et al. (2003) proposed that the hypsometry of
530 catchments correlates to catchment properties. However, the lack of correlation
531 between the hypsometric integral and catchment properties in this study does not
532 support these findings but does support those by Walcott and Summerfield (2008)
533 who also worked in ancient settings. When assessing variation in the western-
534 draining catchments, the hypsometric integral values generally decrease toward the
535 escarpment but show large variation. Regardless of stream order or location,

536 correlation between catchment properties and the hypsometric integral is poor, which
537 was also identified by Walcott and Summerfield (2008). Variation is larger between
538 smaller subcatchments (<4), which is attributed to the smaller subcatchments having
539 had less time to develop or to structural/rock type control having a larger influence
540 on the smaller basins.

541 *5.4. Implications and application of morphometric indices to ancient settings*

542 The Gouritz catchment has had a long history of development since the Mesozoic
543 breakup of Gondwana and the concomitant Cretaceous exhumation of southern
544 South Africa. When assessing morphometric indices, this history needs to be
545 understood, especially as large catchments like the Gouritz do not evolve in a
546 uniform manner (Grimaud et al., 2014) as indicated by the variation in trunk river
547 morphometric indices.

548 The long-lived nature of ancient catchments causes morphometric indices to record
549 the composite effects of multiple factors. This is seen within the hypsometric curve of
550 the Gouritz catchment whereby the middle portion appears to record rock type
551 controls related to inherited structure (Fig. 7) and the lower portion tectonic impacts.
552 Over long timescales, signals can be lost, overprinted, or truncated (Fig. 11), which
553 can also be recorded in the sedimentary history of basins (Jerolmack and Paola,
554 2010; Covault et al., 2013; Romans et al., 2015). The large-scale tectonic event of
555 Gondwana rifting and the debated tectonic uplift history of the catchment since rifting
556 cannot directly be related to morphometric indices in this study (e.g., Walcott and
557 Summerfield, 2008). This is because of the long time for the catchment to respond to
558 and erode the resulting geomorphological impression of the tectonic pulse, coupled
559 with overprinting of other signals (both internal and external; Allen, 2008) and the
560 poorly constrained history of the Gouritz catchment. This is complicated by the lack

561 of understanding of the timescale at which tectonic or climatic factors affect
562 catchments after their initiation and of the response time within the catchment (e.g.
563 Allen, 2008). Overall, the prevailing theories of tectonic and climatic impacts on
564 landscape development cannot be tested properly using morphometric indices in this
565 ancient landscape. The Gouritz catchment has preserved drainage structures (*sensu*
566 Hack, 1960) because of the relatively constant climate since the end of the
567 Cretaceous and lack of tectonic activity. The current planform of the Gouritz is
568 closely linked to rock type, as shown by the hypsometric curves, with steep relief,
569 knickpoints, and high SL in the CFB and subdued relief in the less resistant Karoo
570 Supergroup rock types. Nonetheless, a range of controls will have shaped the
571 Gouritz catchment. However, bedrock geology within these ancient catchments is
572 judged to be the dominant control on the morphometrics as it is the longest lived
573 *relatively* constant boundary condition in comparison to tectonic or climatic change
574 (Fig. 11).

575 **6. Conclusion**

576 Morphometric indices, including stream length gradient and hypsometric integrals,
577 were extracted from the tectonically quiescent Gouritz catchment and confirm that
578 the catchment has had a complicated extended geomorphological history. This is
579 expected for a catchment that has developed since the Jurassic break-up of
580 Gondwana and large-scale exhumation from the Cretaceous onward. Nonetheless
581 with a combined geological-geomorphological approach and analysis across
582 different spatial scales, we are able to decipher that at a catchment scale, indices
583 such as hypsometry are affected by resistant rock types, whereby resistant units
584 preserve topography at a subcatchment and catchment scale. The influence of rock

585 type is scale dependent on river channel long profiles and is more prevalent in
586 catchments of stream orders <4; knickpoints are pinned on boundaries between
587 quartzites and less resistant rock types. Within the larger trunk rivers, stream length
588 gradient is mainly affected by the Uitenhage Group with low values experienced in
589 the upper reaches of the catchment. The trunk rivers dissect the CFB because of
590 their antecedence. Contacts between quartzite and less resistant rock types in these
591 locations are not shown as knickpoints or the highest stream length gradient values,
592 indicating a long duration of development. Control by inherited tectonic structures in
593 this study is therefore mainly seen within smaller subcatchments that drain the CFB
594 as shown by the range in circularity values and within the long profiles of the rivers
595 that cross the CFB

596 Hypsometric curve shape is normally related to external variation in climate or
597 tectonics; however, the sinusoidal hypsometric curve of the Gouritz catchment can
598 be attributed to elevation preservation owing to resistant lithologies and to the
599 preservation of pediments because of low erosion rates. Tectonic influence caused
600 by mantle plumes would cause systematic variation in indices, which is not seen as
601 shown by the lack of correlation between catchment location or stream order.
602 However, large scale differential uplift related to exhumation in the Cretaceous and
603 coastal upwarp because of Mesozoic rifting could still be impacting catchment
604 development, but these controls are hard to distinguish. Within smaller
605 subcatchments, variation in hypsometric curve can be attributed to stream capture in
606 some locations.

607 Overall, morphometric indices allow a first-order characterisation of ancient
608 landscapes and highlight the importance of resistant lithologies. In long-lived
609 catchments, the influence of tectonic activity cannot clearly be ascribed to variation

610 in morphometric indices and appear to be subdued and shredded by the impact of
611 resistant rock types. Caution must therefore be taken when comparing morphometric
612 indices within different tectonic regimes and with different durations of development.
613 Future work should investigate how morphometric indices vary over time in such
614 tectonically quiescent and/or ancient regions and examine how long a tectonic or
615 climatic pulse can be preserved within different environments.

616 **Acknowledgements**

617 The authors would like to thank the Council of Geoscience, South Africa, for
618 providing the geological tiles of the study area under the Academic/Research
619 Licence Agreement. The authors would also like to thank two anonymous reviewers
620 who helped to improve the manuscript and the journal editor Richard Marston.

621 **Reference list**

- 622 Abdelkareem, M., Ghoneim, E., El-Baz, F., Askalany, M., 2012. New insight on
623 paleoriver development in the Nile basin of the eastern Sahara. *J.Afr. Earth*
624 *Sci.* 62, 35-40.
- 625 Allen, P. A., 2008. Time scales of tectonic landscapes and their sediment routing
626 systems. In: Gallagher, K., Jones, S.J., Wainwright, J. (Eds.), *Landscape*
627 *Evolution: Denudation, Climate and Tectonics over Different Time and Space*
628 *Scales*, Geol. Soc. London, Spec. Pub. 296, pp. 7-28.
- 629 Antón, L., De Vicente, G., Muñoz-Martín, A., Stokes, M., 2014. Using river long
630 profiles and geomorphic indices to evaluate the geomorphological signature of
631 continental scale drainage capture, Duero basin (NW Iberia). *Geomorphology*
632 206, 250-261.

- 633 Bakker, E. M. V. Z., Mercer, J. H., 1986. Major late Cainozoic climatic events and
634 palaeoenvironmental changes in Africa viewed in a world wide context.
635 *Palaeogeogr., Palaeoclimatol., Palaeoecol.* 56, 217-235.
- 636 Bar-Matthews, M., Marean, C. W., Jacobs, Z., Karkanas, P., Fisher, E. C., Herries,
637 A. I., Brown, K., Williams, H. M., Bernatchez, J., Ayalon, A., Nilssen, P. J.,
638 2010. A high resolution and continuous isotopic speleothem record of
639 paleoclimate and paleoenvironment from 90 to 53 ka from Pinnacle Point on
640 the south coast of South Africa. *Quat. Sci. Rev.* 29, 2131-2145.
- 641 Bessin, P., Guillocheau, F., Robin, C., Schrötter, J. M., Bauer, H., 2015. Planation
642 surfaces of the Armorican Massif (western France): Denudation chronology of
643 a Mesozoic land surface twice exhumed in response to relative crustal
644 movements between Iberia and Eurasia. *Geomorphology* 233, 75-91.
- 645 Bierman, P. R., Coppersmith, R., Hanson, K., Neveling, J., Portenga, E. W., Rood,
646 D. H., 2014. A cosmogenic view of erosion, relief generation, and the age of
647 faulting in southern Africa. *GSA Today* 24, 4-11.
- 648 Bishop, P., 2007. Long-term landscape evolution: linking tectonics and surface
649 processes. *Earth Surf. Process. Landf.* 32, 329-365.
- 650 Bishop, P., Hoey, T. B., Jansen, J. D., Artza, I. L., 2005. Knickpoint recession rate
651 and catchment area: the case of uplifted rivers in Eastern Scotland. *Earth*
652 *Surf. Process. Landf.* 30, 767-778.
- 653 Brown, R.W., Summerfield, M.A., Gleadow, A.J.W., 2002. Denudation history along
654 a transect across the Drakensberg Escarpment of southern Africa derived
655 from apatite fission track thermochronology. *J. Geophys. Res.* 107, 1-18.
- 656 Burke, K., 1996. The African plate. *S. Afr. J. Geol.*, 99, 341-409.

- 657 Carignano, C., Cioccale, M., Rabassa, J., 1999. Landscape antiquity of the Central
658 Eastern Sierras Pampeanas (Argentina): Geomorphological evolution since
659 Gondwanic times. *Z. Geomorph. Supplement Band 118*, 245–268.
- 660 Chen, Y.C., Sung, Q., Cheng, K.-Y., 2003. Along-strike variations of morphotectonic
661 features in the Western Foothills of Taiwan: tectonic implications based on
662 stream-gradient and hypsometric analysis. *Geomorphology* 56, 109-137.
- 663 Chorley, R. J., 1957. Climate and morphometry. *J. Geol.* 65, 628-638.
- 664 Cockburn, H. A. P., Brown, R. W., Summerfield, M. A., Seidl, M. A., 2000.
665 Quantifying passive margin denudation and landscape development using a
666 combined fission-track thermochronology and cosmogenic isotope analysis
667 approach. *Earth Planet. Sci. Lett.* 179, 429-435.
- 668 Covault, J. A., Craddock, W. H., Romans, B. W., Fildani, A., Gosai, M., 2013. Spatial
669 and temporal variations in landscape evolution: Historic and longer-term
670 sediment flux through global catchments. *J. Geol.* 121, 35-56.
- 671 CSIR., 2007. State of Rivers Report. Rivers of the Gouritz Water Management area
672 2007. Available -
673 http://www.csir.co.za/rhp/state_of_rivers/WCape/gouritz07.pdf
- 674 Dardis, G.F., Beckedahl, H.R., 1991. The role of rock properties in the development
675 of bedrock-incised rills and gullies: examples from southern
676 Africa. *GeoJournal* 23, 35-40.
- 677 Davis, J., 2010. Hypsometric Tools. Available -
678 <http://arcscripts.esri.com/details.asp?dbid=16830>
- 679 Davis, W. M., 1889. The rivers and valleys of Pennsylvania. *Nat. Geogr.*
680 *Mag.* 1, 183-253.
- 681 de Wit, M., 2007. The Kalahari Epeirogeny and climate change: differentiating cause

- 682 and effect from core to space. *S. Afr. J. Geol.* 110, 367-392.
- 683 Dean, W. R. J., Hoffinan, M. T., Meadows, M. E., Milton, S. J., 1995. Desertification
684 in the semi-arid Karoo, South Africa: review and reassessment. *J. Arid*
685 *Environ.* 30, 247-264.
- 686 Decker, J. E., Niedermann, S., De Wit, M. J., 2013. Climatically influenced
687 denudation rates of the southern African plateau: Clues to solving a
688 geomorphic paradox. *Geomorphology* 190, 48-60.
- 689 Demoulin, A., Zárata, M., Rabassa J., 2005. Long-term landscape development: a
690 perspective from the southern Buenos Aires ranges of east central Argentina.
691 *J. S. Am. Earth Sci.* 19, 193–204.
- 692 Dingle, R. V., Hendey, Q. B., 1984. Late Mesozoic and Tertiary sediment supply to
693 the eastern Cape Basin (SE Atlantic) and palaeo-drainage systems in
694 southwestern Africa. *Mar. Geol.* 56, 13-26.
- 695 Doucouré, C.M., de Wit, M.J., 2003. Old inherited origin for the present near bimodal
696 topography of Africa. *J. Afri. Earth Sci.* 36, 371–388.
- 697 Du Toit, A., 1937. *Our Wandering Continents*. Oliver and Boyd, U.K, 366 pp.
- 698 Du Toit, A., 1954. *The Geology of South Africa*, 3rd edn. Oliver and Boyd, U.K.
699 539 pp.
- 700 Duvall, A., Kirby, E., Burbank, D., 2004. Tectonic and lithologic controls on bedrock
701 channel profiles and processes in coastal California. *J. Geophys. Res.: Earth*
702 *Surf.* 109, 1-18.
- 703 Fairbridge, R.W., 1968. *The encyclopedia of geomorphology*. Reinhold Book
704 Corporation, New York, 1295 pp.
- 705 Fleming, A., Summerfield, M. A., Stone, J. O., Fifield, L. K., Cresswell, R. G., 1999.
706 Denudation rates for the southern Drakensberg escarpment, SE Africa,

- 707 derived from in-situ-produced cosmogenic ^{36}Cl : initial results. *J. Geol. Soc.*
708 156, 209-212.
- 709 Flint, S. S., Hodgson, D. M., Sprague, A. R., Brunt, R. L., Van der Merwe, W. C.,
710 Figueiredo, J., Prélat, A., Box, D., Di Celma, C., Kavanagh, J. P., 2011.
711 Depositional architecture and sequence stratigraphy of the Karoo basin floor
712 to shelf edge succession, Laingsburg depocentre, South Africa. *Mar. Petrol.*
713 *Geol.* 28, 658-674.
- 714 Friend, P. F., Jones, N. E., Vincent, S. J., 2009. Drainage evolution in active
715 mountain belts: extrapolation backwards from present-day Himalayan river
716 patterns. In: Smith, N.D., Rogers, J. (Eds). *Fluvial Sedimentology VI*, Blackwell
717 Publishing Ltd., Oxford, UK, pp. 305-313.
- 718 Gallagher, K., Brown, R., 1999. Denudation and uplift at passive margins: the record
719 on the Atlantic Margin of southern Africa. *Philos. Trans. Roy. Soc. London.*
720 *Ser. A: Math., Phys. Eng. Sci.* 357, 835-859.
- 721 Ghosh, P., Sinha, S., Misra, A., 2014. Morphometric properties of the trans-
722 Himalayan river catchments: Clues towards a relative chronology of orogen-
723 wide drainage integration. *Geomorphology* 233, 127-141.
- 724 Gilchrist, A.R., Summerfield, M.A., 1990. Differential denudation and flexural isostasy
725 in formation of rift-margin upwarps. *Nature*, 346, 739-742.
- 726 Gorelov, S.K., Drenev, N.V., Mescheryakov, Y.A., Tikanov, N.A., Fridland, V.M.,
727 1970. Planation surfaces of the USSR. *Geomorphology* 1, 18–29.
- 728 Goudie, A. S., 2005. The drainage of Africa since the Cretaceous. *Geomorphology*
729 67, 437-456.
- 730 Goudie, A.S., 2006. The Schmidt Hammer in geomorphological research. *Prog. Phys.*
731 *Geog.* 30, 703-718.

- 732 Goudie, A., Viles, H., Allison, R., Day, M., Livingstone, I., Bull, P., 1990. The
733 geomorphology of the Napier Range, Western Australia. *Trans. Inst. Brit.*
734 *Geogr.* 15, 308-322.
- 735 Grimaud, J.L., Chardon, D., Beauvais, A., 2014. Very long-term incision dynamics of
736 big rivers. *Earth Planet. Sci. Lett.* 405, 74-84.
- 737 Gunnell, Y., Braucher, R., Bourles, D., André, G., 2007. Quantitative and qualitative
738 insights into bedrock landform erosion on the South Indian craton using
739 cosmogenic nuclides and apatite fission tracks. *Geol. Soc. Am. Bull.* 119, 576-
740 585.
- 741 Gupta, S., 1997. Himalayan drainage patterns and the origin of fluvial megafans in
742 the Ganges foreland basin. *Geology* 25, 11-14.
- 743 Hack, J. T., 1960. Interpretation of erosional topography in humid temperate regions.
744 *Am. J. Sci.* 258-A, 80-97.
- 745 Hack, J. T., 1973. Stream-profile analysis and stream-gradient index. *J. Res. US*
746 *Geol. Sur.* 1, 421-429.
- 747 Hancock, G., Willgoose, G., 2001. Use of a landscape simulator in the validation of
748 the SIBERIA Catchment Evolution Model: Declining equilibrium landforms.
749 *Water Resour. Res.* 37, 1981-1992.
- 750 Hattingh, J., 2008. Fluvial Systems and Landscape Evolution. In: Lewis, C.
751 A. (Ed.). *Geomorphology of the Eastern Cape, South Africa*, NISC, pp. 21-42.
- 752 Hills, E.S., 1963. *Elements of Structural Geology*. Methuen, London, 483 pp.
- 753 Horton, R. E., 1932. Drainage-basin characteristics. *Trans. Am. Geophys. Union* 13,
754 350-361.

- 755 Horton, R. E., 1945. Erosional development of streams and their drainage basins;
756 hydrophysical approach to quantitative morphology. *Geol. Soc. Am. Bull.* 56,
757 275-370.
- 758 Howard, A. D., 1967. Drainage analysis in geologic interpretation: a summation.
759 *AAPG Bull.* 51, 2246-2259.
- 760 Hurtrez, J. E., Sol, C., Lucazeau, F., 1999. Effect of drainage area on hypsometry
761 from an analysis of small-scale drainage basins in the Siwalik Hills (Central
762 Nepal). *Earth Surf. Process. Landf.* 24, 799-808.
- 763 Jansen, J. D., Codilean, A. T., Bishop, P., Hoey, T. B., 2010. Scale dependence of
764 lithological control on topography: Bedrock channel geometry and catchment
765 morphometry in western Scotland. *J. Geol.* 118, 223-246.
- 766 Jerolmack, D. J., Paola, C., 2010. Shredding of environmental signals by sediment
767 transport. *Geophys. Res. Lett.* 37, 1-5.
- 768 Keller, E.A., Pinter, N., 2002. *Active tectonics: Earthquakes, Uplift and Landscape-*
769 *Second Edition.* Prentice Hall, New Jersey, 362 pp.
- 770 King, L.C., 1951. *South African Scenery.* 2nd edn. Oliver and Boyd, U.K, pp. 379.
- 771 King, L. C., 1953. Canons of landscape evolution. *Geol. Soc. Am. Bull.* 64, 721-752.
- 772 King, L.C., 1956a. A geomorphological comparison between Brazil and South Africa.
773 *Q. J. Geol. Soc.* 112, 445–474.
- 774 King, L.C., 1956b. A geomorfologia do Brasil oriental. *Rev. Bras. Geogr.* 18,186–
775 263.
- 776 King, L.C., 1963. *South African Scenery.* Oliver and Boyd, London, United Kingdom,
777 308 pp.
- 778 King, L.C., 1972. *The Natal monocline: explaining the origin and scenery of Natal,*
779 *South Africa.* Geology Department, University of Natal, South Africa, 113 pp.

- 780 Knighton, D., 1998. Fluvial forms and processes: a new perspective. Routledge,
781 400 pp.
- 782 Kounov, A., Niedermann, S., De Wit, M. J., Viola, G., Andreoli, M., Erzinger, J.,
783 2007. Present denudation rates at selected sections of the South African
784 escarpment and the elevated continental interior based on cosmogenic ^3He
785 and ^{21}Ne . *S. Afr. J. Geol.* 110, 235-248.
- 786 Kounov, A., Viola, G., De Wit, M., Andreoli, M. A. G., 2009. Denudation along the
787 Atlantic passive margin: new insights from apatite fission-track analysis on the
788 western coast of South Africa. In: Lisker, F., Ventura, B., Glasmacher, U.A
789 (Eds.), *Thermochronological Methods: From Palaeotemperature Constraints to*
790 *Landscape Evolution Models*, Geol. Soc. London, Spec. Publ. 324, 287-306.
- 791 Kounov, A., Niedermann, S., de Wit, M. J., Codilean, A. T., Viola, G., Andreoli, M.,
792 Christl, M., 2015. Cosmogenic ^{21}Ne and ^{10}Be reveal a more than 2 Ma Alluvial
793 Fan Flanking the Cape Mountains, South Africa. *S. Afr. J. Geol.* 118, 129-144.
- 794 Lidmar-Bergström, K., 1988. Exhumed cretaceous landforms in south Sweden. *Z.*
795 *Geomorph. Supplement Band 72*, 21–40.
- 796 Manjoro, M. 2015. Structural control of fluvial drainage in the western domain of the
797 Cape Fold Belt, South Africa. *J. Afr. Earth Sci.* 101, 350-359.
- 798 Midgley, G. F., Hannah, L., Millar, D., Thuiller, W., Booth, A., 2003. Developing
799 regional and species-level assessments of climate change impacts on
800 biodiversity in the Cape Floristic Region. *Biol. Cons.* 112, 87-97.
- 801 Miller, V.C., 1953. A Quantitative Geomorphic Study of Drainage Basin
802 Characteristics in the Clinch Mountain Area. New York. Columbia University,
803 Virginia and Tennessee, Project. NR, Technical Report, 389-402.

- 804 Montgomery, D. R., Balco, G., Willett, S. D., 2001. Climate, tectonics, and the
805 morphology of the Andes. *Geology* 29, 579-582.
- 806 Moore, A., Blenkinsop, T., 2002. The role of mantle plumes in the development of
807 continental-scale drainage patterns: the southern African example revisited. *S.*
808 *Afr. J. Geol.* 105, 353-360.
- 809 Moore, A., Blenkinsop, T., 2006. Scarp retreat versus pinned drainage divide in the
810 formation of the Drakensberg escarpment, southern Africa. *S. Afr. J. Geol.*
811 109, 599-610.
- 812 Moore, A., Blenkinsop, T., Cotterill, F. W., 2009. Southern African topography and
813 erosion history: plumes or plate tectonics? *Terra Nova* 21, 310-315.
- 814 Ohmori, H., 1993. Changes in the hypsometric curve through mountain building
815 resulting from concurrent tectonics and denudation. *Geomorphology* 8, 263-
816 277
- 817 Ollier, C., 1991. *Ancient landscapes*. Belhaven Press, London/New York, 233 pp.
- 818 Ollier, C., Pain, C. 2000. *The origin of mountains*. Routledge, London/New York, 345
819 pp.
- 820 Özbek, A., 2009. Variation of Schmidt hammer values with imbrication direction in
821 clastic sedimentary rocks. *Int. J. Rock Mech. Min. Sci.* 46, 548-554.
- 822 Panario, D., Gutiérrez, O., Sánchez Bettucci, L., Peel, E., Oyhançabal, P., Rabassa,
823 J., 2014. Ancient landscapes of Uruguay. In: Rabassa, J., Ollier, C. (Eds.)
824 *Gondwana landscapes in southern South America*, pp. 161–199.
- 825 Partridge, T.C., 1998. Of diamonds, dinosaurs and diastrophism: 150 million
826 years of landscape evolution in southern Africa. *S. Afr. J. Geol.* 101, 165–184.
- 827 Partridge, T. C., Maud, R. R., 1987. Geomorphic evolution of southern Africa since
828 the Mesozoic. *S. Afr. J. Geol.* 90, 179-208.

- 829 Paton, D. A., 2006. Influence of crustal heterogeneity on normal fault dimensions
830 and evolution: southern South Africa extensional system. *J. Struct. Geol.* 28,
831 868-886.
- 832 Peulvast, J. P., Bétard, F., 2015. A history of basin inversion, scarp retreat and
833 shallow denudation: The Araripe basin as a keystone for understanding long-
834 term landscape evolution in NE Brazil. *Geomorphology* 233, 20-40.
- 835 Prince, P. S., Spotila, J. A., Henika, W. S., 2011. Stream capture as driver of
836 transient landscape evolution in a tectonically quiescent setting. *Geology* 39,
837 823-826.
- 838 Richards, K., 1982. *Rivers, Form and Processes in Alluvial channels*. London:
839 Methuen, 358 pp.
- 840 Rogers, C. A., 1903. The geological history of the Gouritz River system. *Trans. S.*
841 *Afr. Philos. Soc.* 14, 375-384.
- 842 Romans, B. W., Castelltort, S., Covault, J. A., Fildani, A., Walsh, J. P., 2015.
843 Environmental signal propagation in sedimentary systems across
844 timescales. *Earth-Sci. Rev.* DOI: 10.1016/j.earscirev.2015.07.012
- 845 Rust, D.J., Summerfield, M.A., 1990. Isopach and borehole data as indicators of
846 rifted margin evolution in southwestern Africa. *Mar. Petrol. Geol.* 7, 277-287.
- 847 Scharf, T. E., Codilean, A. T., de Wit, M., Jansen, J. D., Kubik, P., W. 2013. Strong
848 rocks sustain ancient postorogenic topography in southern Africa. *Geology* 41,
849 331-334.
- 850 Schumm, S. A., 1956. Evolution of drainage systems and slopes in badlands at
851 Perth Amboy, New Jersey. *Geol. Soc. Am. Bull.* 67, 597-646.

- 852 Seydack, A. H., Bekker, S. J., Marshall, A. H. 2007. Shrubland fire regime scenarios
853 in the Swartberg Mountain Range, South Africa: Implications for fire
854 management. *Int. J. Wildland Fire* 16, 81-95.
- 855 Shelton, C. M., 2015. Rebound hardness results for raw material located near
856 Pinnacle Point, South Africa and the implications thereof. Ma Thesis, The
857 University of Texas, America.
- 858 Sklar, L. S., Dietrich, W. E., 2001. Sediment and rock strength controls on river
859 incision into bedrock. *Geology* 29, 1087-1090.
- 860 Snyder, N. P., Whipple, K. X., Tucker, G. E., Merritts, D. J., 2000. Landscape
861 response to tectonic forcing: Digital elevation model analysis of stream
862 profiles in the Mendocino triple junction region, northern California. *Geol. Soc.
863 Am. Bull.* 112, 1250-1263.
- 864 Spikings, A. L., Hodgson, D. M., Paton, D. A., Sychala, Y. T., 2015. Palinspastic
865 restoration of an exhumed deep-water system: a workflow to improve
866 paleogeographic reconstructions. *Interpretation*, 3, SAA71-SAA87
867 <http://dx.doi.org/10.1190/INT-2015-0015.1>
- 868 Strahler, A. N., 1952. Hypsometric (Area-Altitude) Analysis of Erosional Topography.
869 *Geol. Soc. Am. Bull.* 63, 1117.
- 870 Strahler, A. N., 1957. Quantitative analysis of watershed geomorphology. *J. Civil Eng.*
871 101, 1258-1262.
- 872 Strahler, A.N., 1964. Quantitative geomorphology of drainage basins and channel
873 networks. In: V. T. Chow (Ed), *Handbook of Applied Hydrology*. McGraw Hill
874 Book Company, New York, pp. 39-76.
- 875 Summerfield, M. A., 1991. *Global geomorphology*. Routledge, pp. 537

- 876 Tankard, A., Welsink, H., Aukes, P., Newton, R., Stettler, E., 2009. Tectonic
877 evolution of the Cape and Karoo basins of South Africa. *Mar. Petrol. Geol.* 26,
878 1379-1412.
- 879 Tinker, J., De Wit, M., Brown, R., 2008a. Mesozoic exhumation of the southern
880 Cape, South Africa, quantified using apatite fission track thermochronology.
881 *Tectonophysics* 455, 77-93.
- 882 Tinker, J., de Wit, M., Brown, R., 2008b. Linking source and sink: evaluating the
883 balance between onshore erosion and offshore sediment accumulation since
884 Gondwana break-up, South Africa. *Tectonophysics* 455, 94-103.
- 885 Tinkler, K., Wohl, E., 1998. A primer on bedrock channels. In: Tinkler, K.J., Wohl,
886 E.E. (Eds.), *Rivers over rock: Fluvial processes in bedrock channels*, pp. 1-18.
- 887 Tooth, S., Brandt, D., Hancox, P. J., McCarthy, T. S., 2004. Geological controls on
888 alluvial river behaviour: a comparative study of three rivers on the South
889 African Highveld. *J. Afr. Earth Sci.* 38, 79-97.
- 890 Twidale, C. R., 2007a. *Ancient Australian Landscapes*. Rosenberg Pub Pty Limited,
891 144 pp.
- 892 Twidale, C.R., 2007b. Bornhardts and associated fracture patterns. *Rev.*
893 *Asoc. Geol. Argent.* 62, 139–153.
- 894 van der Beek, P., Summerfield, M.A., Braun, J., Brown, R. W., Fleming, A.,
895 2002. Modelling post breakup landscape development and denudational
896 history across the southeastern African (Drakensberg Escarpment) margin. *J.*
897 *Geophys. Res.* 107, B12.
- 898 Walcott, R. C., Summerfield, M. A., 2008. Scale dependence of hypsometric
899 integrals: An analysis of southeast African basins. *Geomorphology* 96, 174-
900 186.

- 901 Whipple, K. X., 2004. Bedrock rivers and the geomorphology of active orogens.
902 Annu. Rev. Earth Planet. Sci. 32, 151-185.
- 903 Zernitz, E. R., 1932. Drainage patterns and their significance. J. Geol. 40, 498-521.
- 904 Zhang, W., Oguchi, T., Hayakawa, Y. S., Peng, H., 2013. Morphometric analyses of
905 Danxia landforms in relation to bedrock geology: a case of Mt. Danxia,
906 Guangdong Province, China. Open Geol. J. 7, 54-62.
- 907

908 Figure Captions

909

910 **Table 1**

911 Variation in drainage density for the main lithological groups of the Gouritz
 912 catchment

Lithology	Drainage density (km/km²)
Igneous intrusions	0.28
Quartzites	0.23
Cango Cave group	0.37
Uitenhage group	0.35
Karoo Supergroup	0.44
Cape Supergroup	0.37

913

914 **Table 2**

915 *Linear aspects of the Gouritz catchment*

Stream order	Stream number	Average stream length (km)	Bifurcation ratio
1	2811	5.36	3.45
2	814	9.29	3.86

3	211	17.51	3.91
4	54	30.01	6.00
5	9	117.77	4.50
6	2	52.44	2.00
7	1	355.96	
Mean			3.39

916

917 **Table 3**

918 *Variation in hypsometric integral in the western-draining catchments with stream*

919 *order*

Stream order	N	Highest hypsometric integral	Lowest hypsometric integral	Mean	Range	Standard deviation
1	18	0.53	0.32	0.43	0.21	0.62
2	13	0.69	0.27	0.43	0.42	0.11
3	13	0.51	0.23	0.38	0.27	0.75
4	3	0.38	0.18	0.30	0.20	0.10
5	1			0.24		
6	2			0.30		

920

921 **Table 4**

922 *Variation in hypsometric integral with catchment location*

Location	N	Highest hypsometric integral	Lowest hypsometric integral	Mean	Range	Standard deviation
Coastal	7	0.69	0.19	0.35	0.50	0.17
Cape Fold Belt	14	0.56	0.30	0.41	0.26	0.07
Central Karoo	28	0.53	0.25	0.41	0.28	0.07

923

924 **Fig. 1.** *The location of the Gouritz catchment in southern South Africa and the six*
 925 *major tributaries and major extension faults. A simplified geological map is also*
 926 *shown highlighting the main rock types.*

927

928 **Fig. 2.** *(A) Topography variation within the Gouritz catchment showing the main*
 929 *physiographic regions; (B) Hammond's landform classification map indicating the*
 930 *catchment is dominated by plains and mountains.*

931

932

933 **Fig. 3.** *Relative resistance of rock types within the Gouritz catchment. Quartzite*
 934 *(Table Mountain Group) and dolerites are the most resistant rock types. The values*
 935 *indicate Schmidt hammer results from the study area, italicised numbers are from*

936 *published studies of the same rock type (1 – Özbek, 2009; 2 – Dardis and Beckedahl*
937 *1991; 3 – Goudie, 2006; 4 – Shelton, 2015; 5 - Goudie et al., 1990).*

938

939 **Fig. 4.** *(A) Drainage pattern of the Cape Fold Belt and Coastal physiographic region,*
940 *showing stream order 3 streams categorised by shape. See Fig. 1 for location. (B)*
941 *and (C) show evidence of stream capture and linear streams confined by folding.*

942

943 **Fig. 5.** *Long profiles of the Gouritz catchment and main tributaries: (A) Buffels River,*
944 *(B) Touws River, (C) Olifants River, (D) Traka River, (E) Gamka River and (F) Dwyka*
945 *River.*

946

947 **Fig. 6.** *Normalised stream length gradient and the relationship to simplified geology*
948 *within the Gouritz catchment. The locations of knickpoints within the smaller*
949 *catchments of the Swartberg range are also shown.*

950

951 **Fig. 7.** *The sinusoidal hypsometric curve of the Gouritz catchment.*

952

953 **Fig. 8.** *Relationship between location, catchment properties, and hypsometric*
954 *integral: (A) area, (B) circularity, (C) relief, (D) dissection, and (E) distance from*
955 *mouth of Gouritz River. The R^2 values indicate no correlation between catchment*
956 *properties and hypsometric integral.*

957

958 **Fig. 9.** (A) Distribution of 'type' curves (straight, convex, concave, and sinusoidal)
959 where RA is relative area and RE is relative elevation; (B) variation in curve shape
960 toward the escarpment. Data extracted from every fifth catchment: (C) area of
961 catchments below 50% of the maximum elevation within the basin; (D) the average
962 lengths of stream order 1 to 6 streams draining the Western Cape.

963

964 **Fig. 10.** Hypsometric curves and lithostratigraphic units for stream order 1-6 (A-F)
965 catchments draining the western side of the Gouritz catchment. Inflection points in
966 the curve are highlighted. The numbers indicate the gradient of each section,
967 delineated by a change in curve shape.

968

969 **Fig. 11.** Synthesis diagram showing the differences between young and ancient
970 catchments and the impact on morphometric indices. Within young landscapes,
971 recent tectonic activity is represented as knickpoints and straight hypsometric
972 curves. However, in ancient catchments this signal is diminished, resulting in pinned
973 knickpoints on lithological divides, sinusoidal curves, and composite effects of
974 multiple factors that make it hard to distinguish dominant controls.

975

976

977

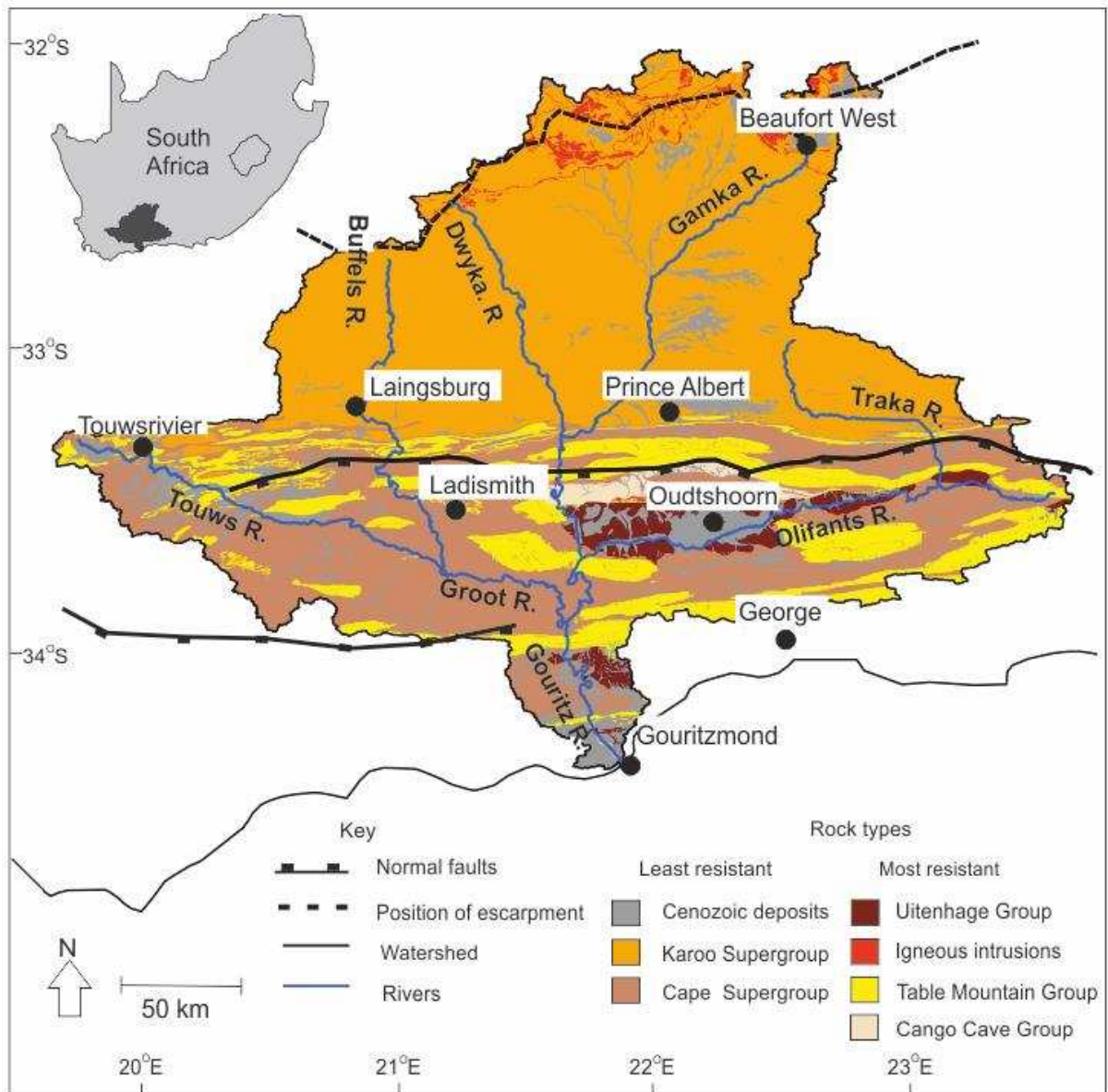
978

979

980

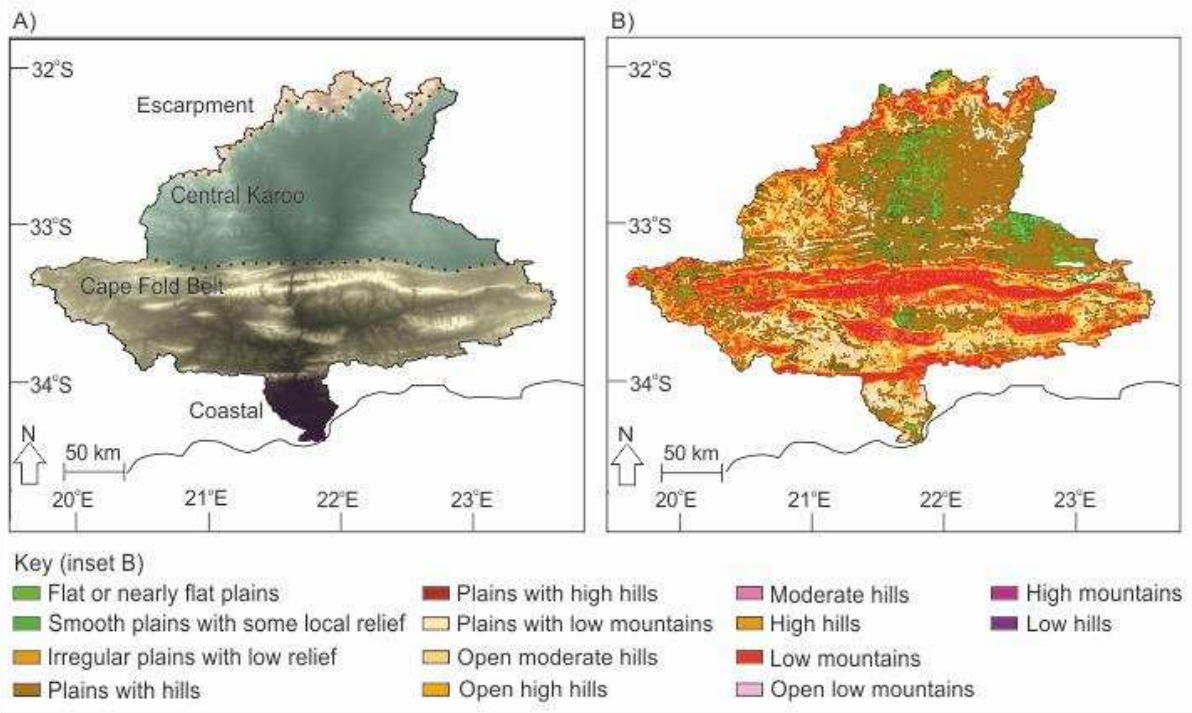
981

982 Figure 1



983
 984
 985
 986
 987
 988
 989
 990
 991

992 Figure 2



993

994

995

996

997

998

999

1000

1001

1002

1003

1004

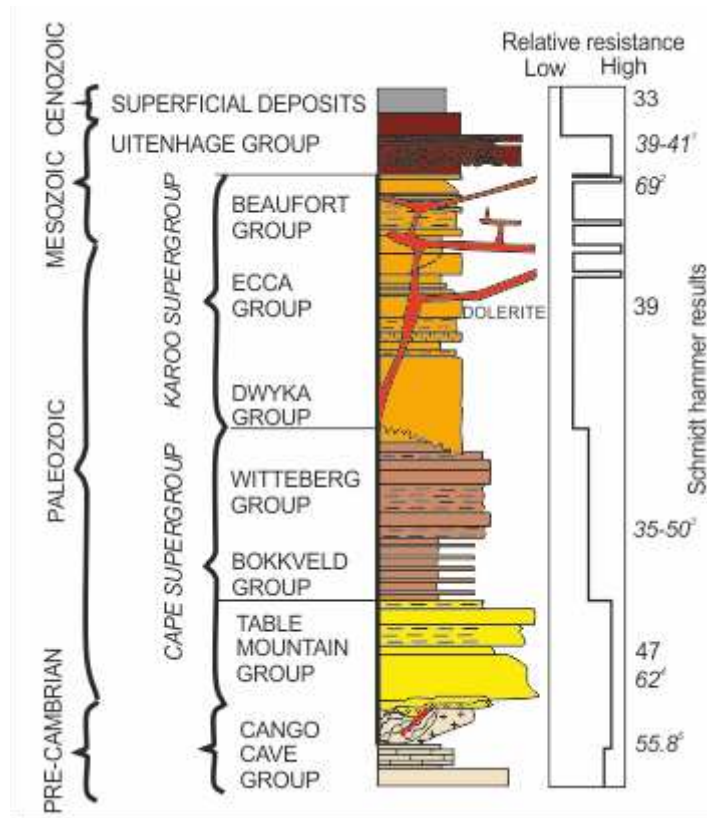
1005

1006

1007

1008

1009 Figure 3



1010

1011

1012

1013

1014

1015

1016

1017

1018

1019

1020

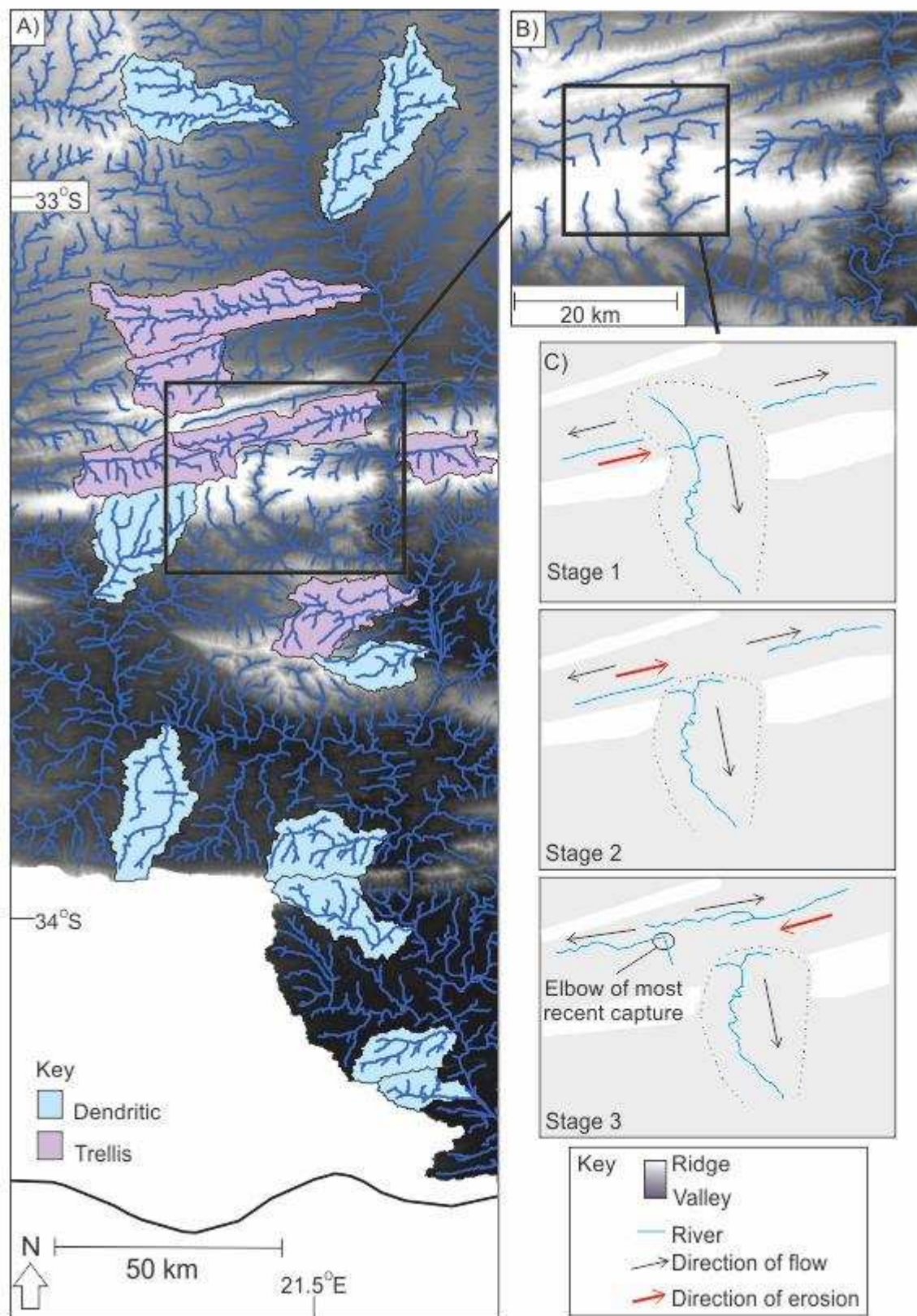
1021

1022

1023

1024

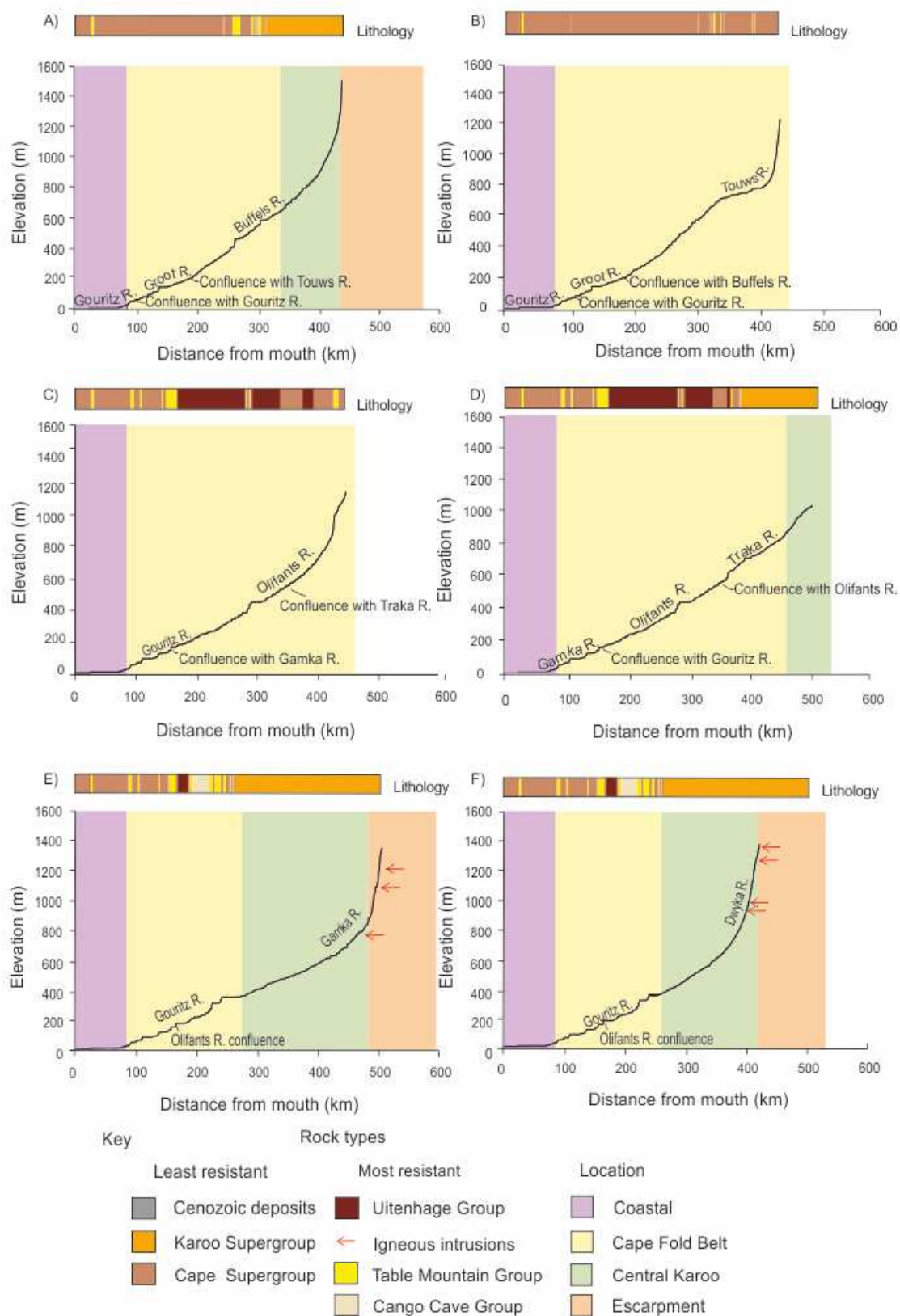
1025 Figure 4



1026

1027

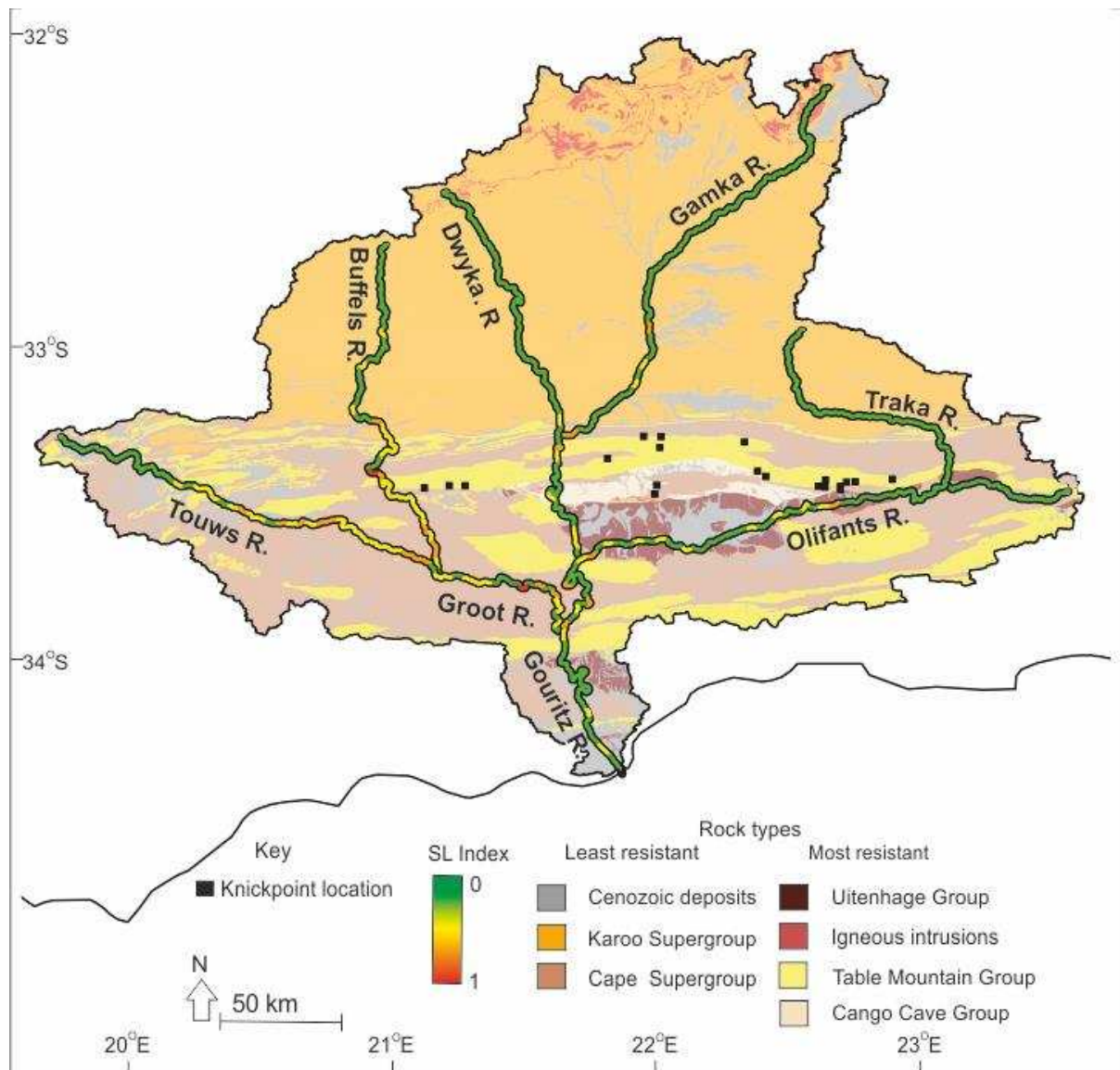
1028 Figure 5



1029

1030

1031 Figure 6



1032

1033

1034

1035

1036

1037

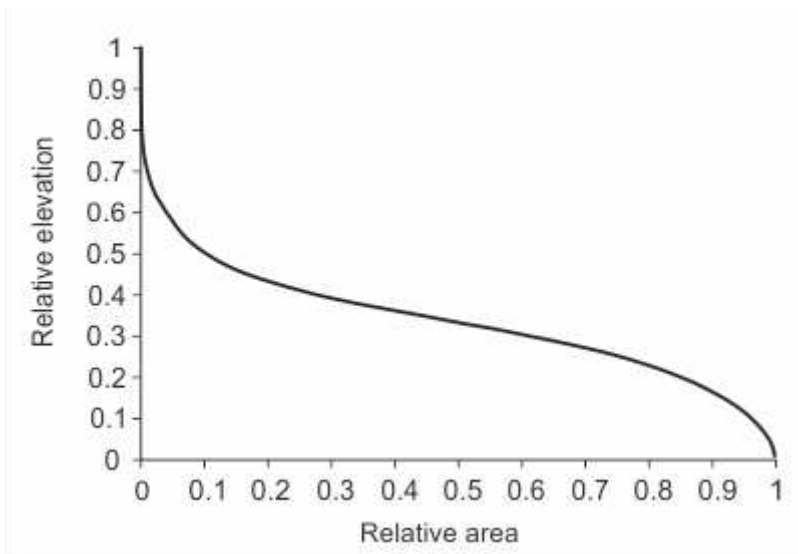
1038

1039

1040

1041

1042 Figure 7



1043

1044

1045

1046

1047

1048

1049

1050

1051

1052

1053

1054

1055

1056

1057

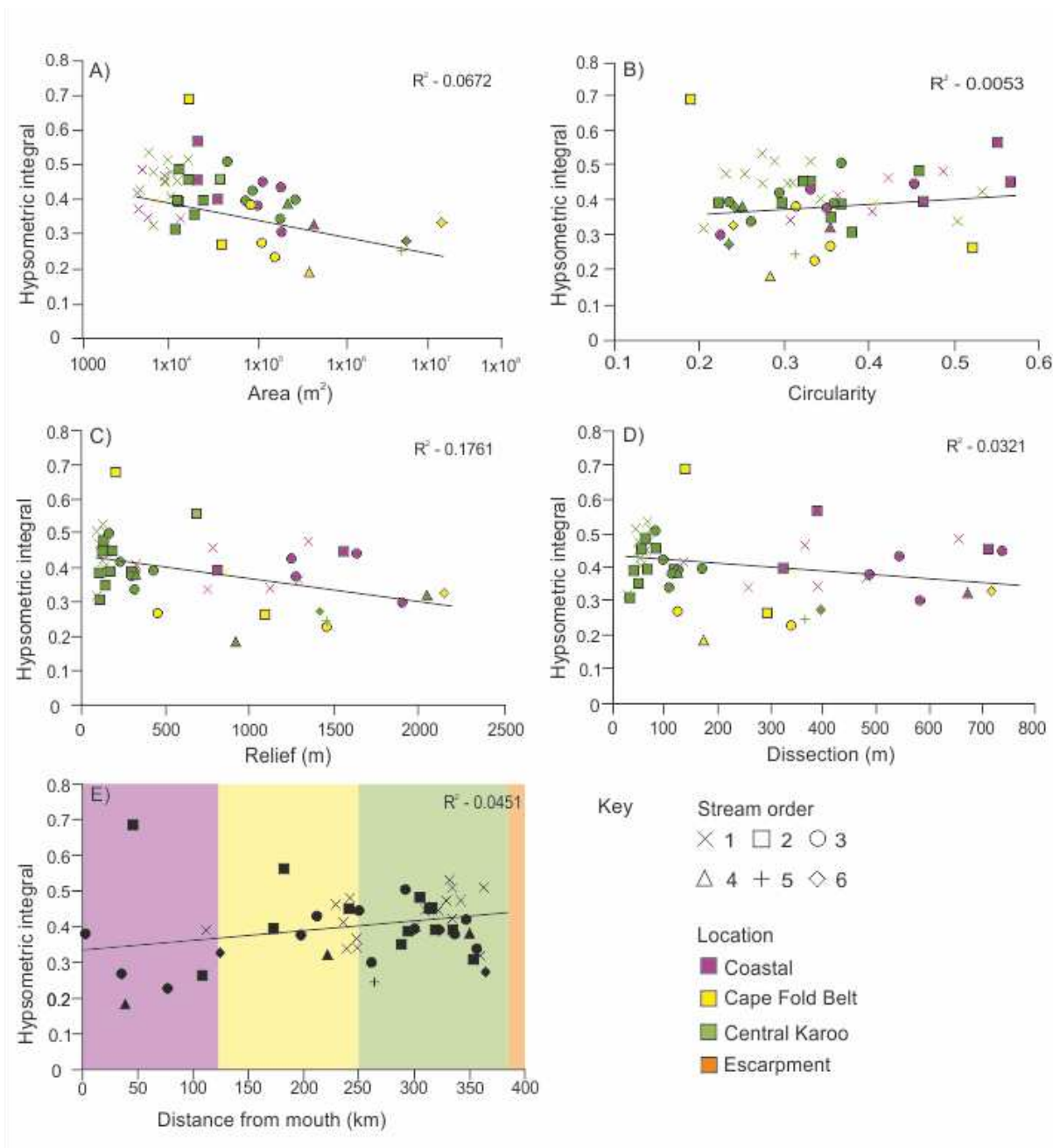
1058

1059

1060

1061

1062 Figure 8



1063

1064

1065

1066

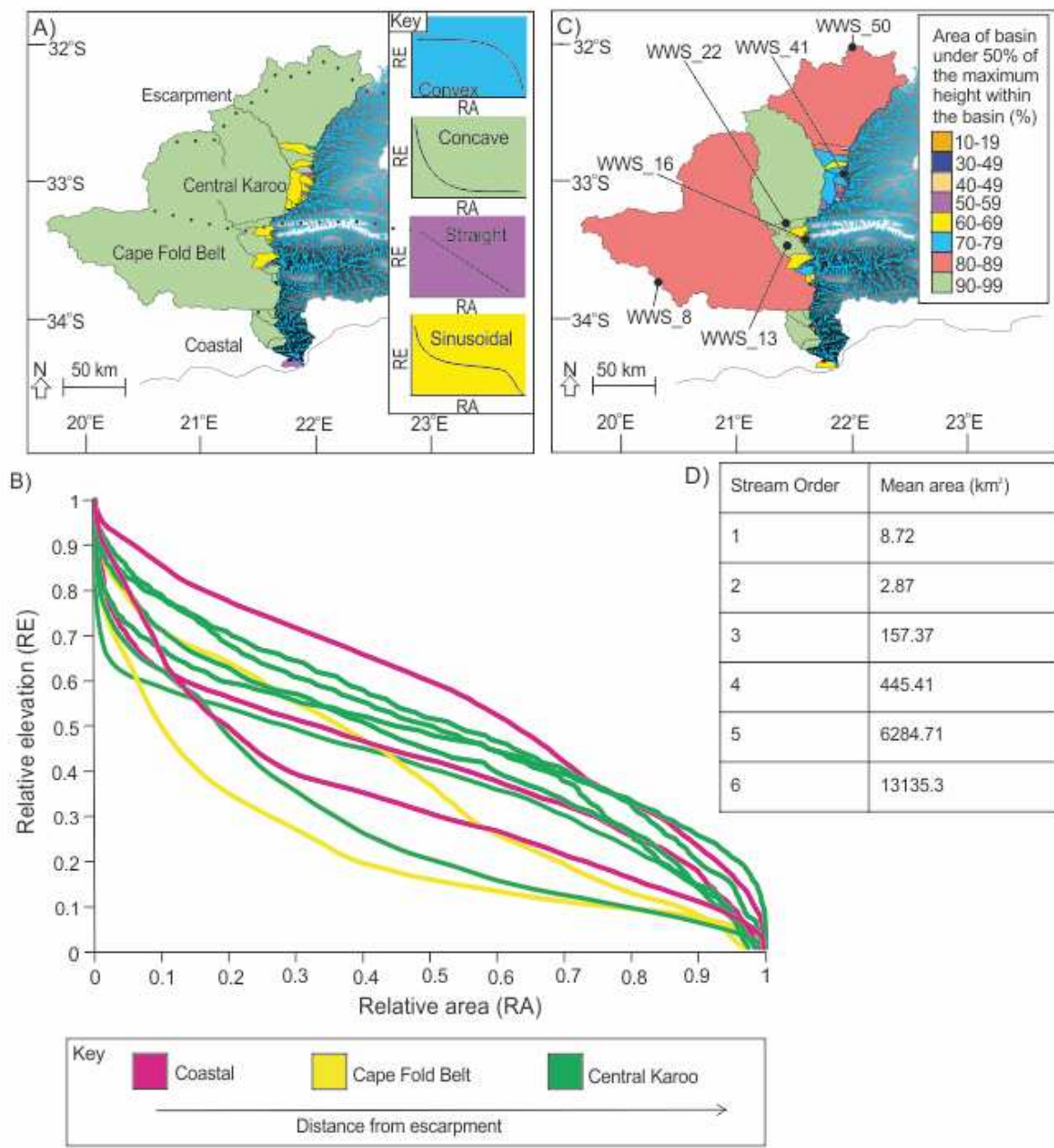
1067

1068

1069

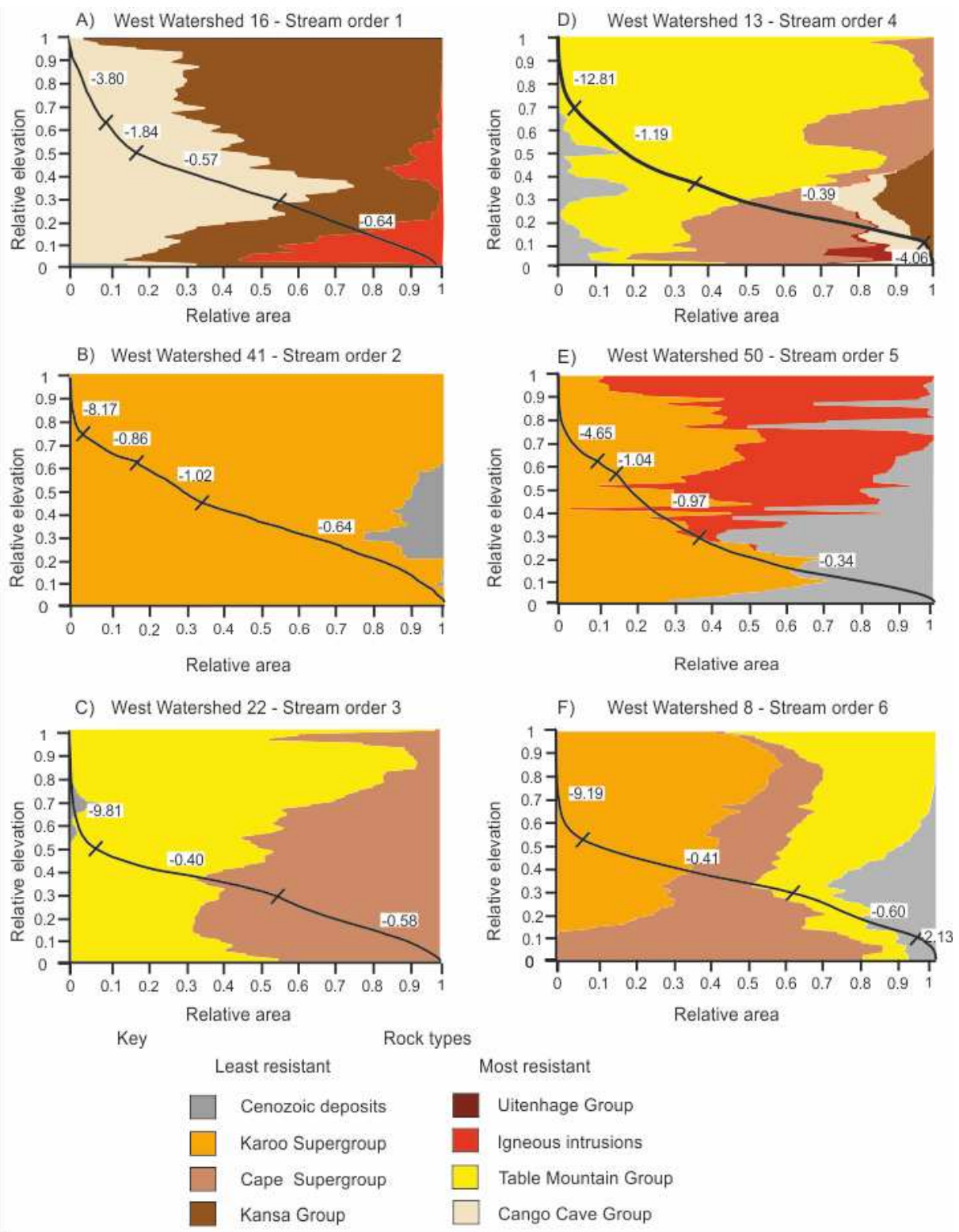
1070

1071 Figure 9



1072
 1073
 1074
 1075
 1076
 1077
 1078
 1079

1080 Figure 10



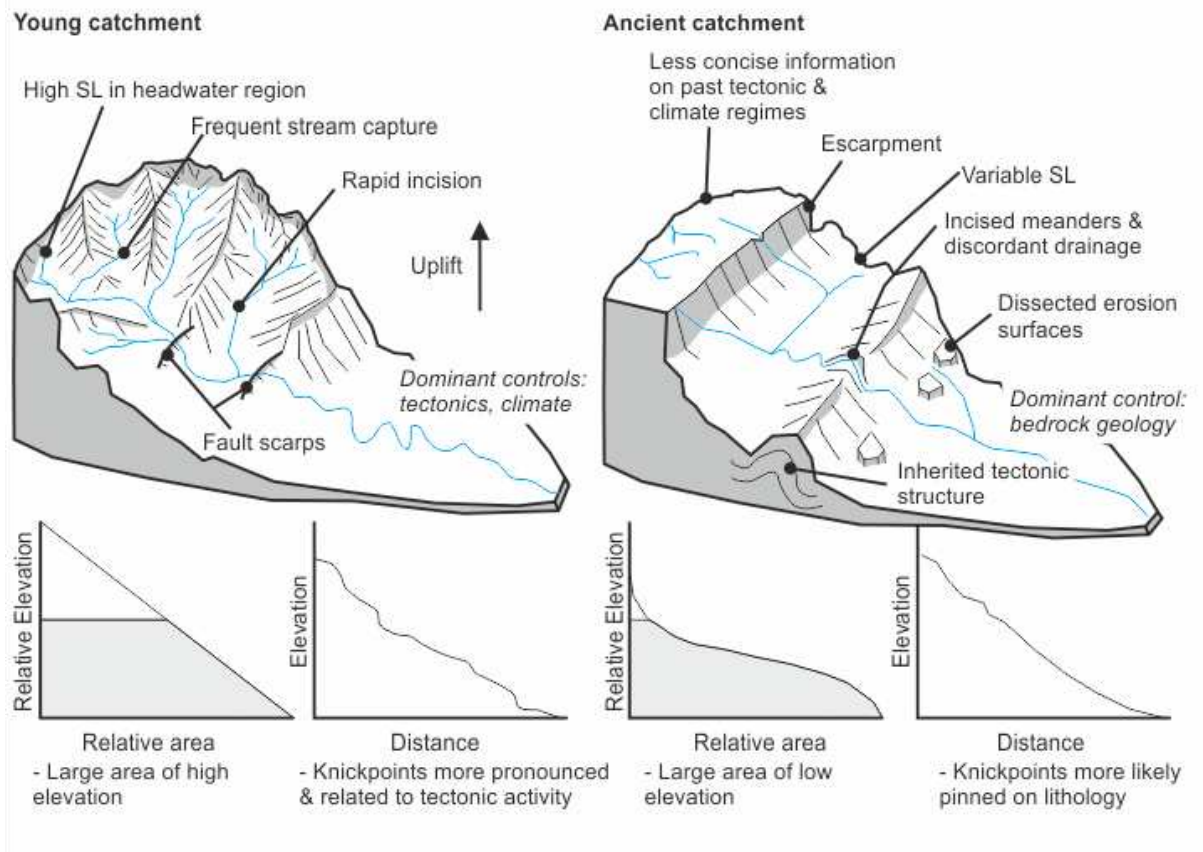
1081

1082

1083

1084

1085 Figure 11



1086